HHS Public Access

Author manuscript

Sci Immunol. Author manuscript; available in PMC 2023 July 10.

Published in final edited form as:

Sci Immunol. 2023 March 17; 8(81): eadc9417. doi:10.1126/sciimmunol.adc9417.

A Mast Cell-Thermoregulatory Neuron Circuit Axis Regulates Hypothermia in Anaphylaxis

Chunjing Bao[1,*], **Ouyang Chen**[2,3], **Huaxin Sheng**[4], **Jeffrey Zhang**[1], **Yikai Luo**[5,6], **Byron W. Hayes**[1], **Han Liang**[5,6,7], **Wolfgang Liedtke**[8,9], **Ru-Rong Ji**[2,3,10], **Soman N. Abraham**[1,11,12,13,*]

[1]Department of Pathology, Duke University Medical Center, Durham, NC 27710, USA

[2]Center for Translational Pain Medicine, Department of Anesthesiology, Duke University Medical Center, Durham, NC 27710, USA

[3]Department of Cell Biology, Duke University Medical Center, Durham, NC 27710, USA

[4]Multidisciplinary Neuroprotection Laboratories, Center of Perioperative Organ Protection, Department of Anesthesiology, Duke University Medical Center, Durham, NC 27710, USA

[5]Graduate Program in Quantitative and Computational Biosciences, Baylor College of Medicine, Houston, TX 77030, USA

[6]Department of Bioinformatics and Computational Biology, The University of Texas MD Anderson Cancer Center, Houston, TX 77030, USA

[7]Department of Systems Biology, The University of Texas MD Anderson Cancer Center, Houston, TX 77030, USA

[8]Department of Neurology, Duke University Medical Center, Durham, NC 27710, USA

[9]Department of Molecular Pathobiology, College of Dentistry, New York University, New York NY 10010

[10]Department of Neurobiology, Duke University Medical Center, Durham, NC 27710, USA

[11]Department of Immunology, Duke University Medical Center, Durham, NC 27710, USA

[12]Department of Molecular Genetics and Microbiology, Duke University Medical Center, Durham NC 27710, USA

[13]Program in Emerging Infectious Diseases, Duke-National University of Singapore, Singapore 169857, Singapore.

Abstract

[*]**Corresponding authors:** Soman N. Abraham: soman.abraham@duke.edu, Chunjing Bao: cb453@duke.edu.

Author Contributions: Studies were designed by C.B., O.C., B.H., R.R.J., W.L. and S.N.A.; C.B, O.C., H.S. and J.Z. carried out experiments. Experimental data was analyzed by C.B. and O.C. with advice from R.R.J., W.L., and S.N.A.; sequencing data was analyzed by Y.L. with advice from H.L.. The manuscript was primarily written by C.B. and S.N.A. All authors contributed to discussions and manuscript review.

Competing interests: W.L. is a full-time executive employee of Regeneron Pharmaceuticals (Tarrytown NY). W.L. owns stock and stock options in Regeneron. The other authors declare that they have no competing interests.

IgE-mediated anaphylaxis is an acute life-threatening systemic reaction to allergens including certain foods and venoms. Anaphylaxis is triggered when blood-borne allergens activate IgE-bound perivascular mast cells (MCs) throughout the body causing extensive systemic release of MC mediators. Through precipitating vasodilatation and vascular leakage, these mediators are believed to trigger a sharp drop in blood pressure in humans and core body temperature in animals. Here we report that the IgE/MC-mediated drop in body temperature in mice associated with anaphylaxis also requires the body's thermoregulatory neural circuit. This circuit is activated when granule-borne chymase from MCs is deposited on proximal TRPV1$^+$ sensory neurons and stimulates them via protease-activated receptor-1 (PAR1). This triggers the activation of the body's thermoregulatory neural network which rapidly attenuates brown adipose tissue (BAT) thermogenesis to cause hypothermia. Mice deficient in either chymase or TRPV1 exhibited limited IgE-mediated anaphylaxis and in wild-type (WT) mice, anaphylaxis could be recapitulated simply by systemically activating TRPV1$^+$ sensory neurons. Thus, in addition to their well-known effects on the vasculature, MCs products, especially chymase, promote IgE-mediated anaphylaxis by activating the thermoregulatory neural circuit.

One-sentence summary:

Anaphylaxis-induced hypothermia depends on mast cell chymase activating TRPV1$^+$ sensory neurons to attenuate thermogenesis by brown fat.

Introduction

IgE-mediated anaphylaxis is a life-threatening immune reaction to diverse allergens found in food, venom and commonly used drugs including antibiotics. In the U.S, as many as 1.6% to 5.1% of the population has experienced this type of allergic reaction with an apparently growing incidence(1). The primary symptoms of anaphylaxis are a sharp drop in blood pressure in humans or a drop in core body temperature in experimental animals, which can be fatal. Intramuscular injection of epinephrine is the only standard intervention, which acts primarily by rapidly constricting blood vessels to restore blood pressure. However, it is now becoming clear that epinephrine may have other additional effects which can help combat other less-known aspects of anaphylaxis(2, 3). Despite the life-threatening nature of IgE-mediated anaphylaxis, there are currently no effective preventative therapeutic options for this allergic reaction.

Mast cells (MCs) are the primary immune cells implicated in IgE-mediated anaphylaxis(4, 5). These cells lie in close proximity to the vasculature all over the body and in this location readily absorb circulating allergen-specific IgE molecules(6). Subsequently, when allergens enter the circulation following ingestion or an insect bite, these IgE-bound MCs become activated, triggering the release of a myriad of prestored inflammatory mediators, including histamine, TNF, platelet-activating factor, proteases, etc. (5). These MC-derived agents, acting alone or in combination, are believed to induce both dilation of blood vessels and vascular leakage. When MCs throughout the body rapidly release a large bolus of mediators into the circulation, a sharp drop in blood pressure and/or core body temperature results(7, 8). MC activation occurs when blood-borne allergens are initially sampled by perivascular dendritic cells and conveyed to perivascular MCs via microvesicles(8). The principal role

of MCs and their products in promoting anaphylaxis was deduced from findings that IgE-sensitized and MC-depleted mice, unlike their wild-type (WT) counterparts, failed to exhibit anaphylaxis when exposed to allergens(8). Additionally, administration of MC products such as histamine into mice caused anaphylaxis-like responses, including blood vessel dilation, increased vascular permeability and rapid drop in core body temperature(9, 10).

A principal regulator of normal body temperature is the thermoregulatory neural circuit, which continuously maintains thermal homeostasis(11). Peripheral feeders into this thermoregulatory central network are thermosensitive peripheral sensory neurons in the dorsal root ganglion (DRG), trigeminal ganglion (TG) and nodose ganglion, etc., with their projections innervating surfaces or viscera, constantly monitoring thermal cues. These primary thermosensitive neurons then project via the spinal cord to the lateral parabrachial nucleus (LPB) in the brainstem, which project to the thermoregulatory centers in the preoptic area (POA) directly rostral to the hypothalamus(11, 12). Following the activation of the POA thermoregulatory centers, downstream effectors are triggered to either increase or decrease heat production and/or heat dissipation to re-establish thermal homeostasis(11). In mice, upon exposure to heat, the POA directs the decrease of BAT thermogenesis and promotes increased dilation of skin blood vessels (e.g., ear, tail blood vessels); whereas, upon cold challenge, BAT thermogenesis is increased while skin blood vessels constrict, and sometimes skeletal muscle shivering is also triggered(11). Considering the magnitude and rapid dynamics of the temperature change evoked in mice during IgE-mediated anaphylaxis, we hypothesized that the thermoregulatory neural circuit could be a contributor to this response, and importantly with key input from peripheral afferents which are anatomically closely associated with MCs across the body. Here, we describe studies examining if MC mediators could impact the body's thermoregulatory neural circuit during IgE-mediated anaphylaxis in mice. We report, as key co-contributors, $TRPV1^+$ peripheral thermosensory neurons feed into this central mechanism, and the MC-secreted mediator chymase can directly activate the $TRPV1^+$ sensory neurons through its receptor, protease-activated receptor-1 (PAR1).

Results

Neuronal modulation in anaphylaxis-associated hypothermia

IgE-mediated anaphylaxis can be induced in mice by sensitizing with TNP-specific IgE, followed by challenge with the allergen, TNP-OVA, 18 hours later (Fig. S1A). Before investigating the possible neuronal involvement in IgE-mediated anaphylaxis, we sought to confirm the pivotal role of MCs in our mouse model. We compared anaphylaxis in IgE-sensitized wild type (WT) and MC-depleted mice and found that only the former experienced anaphylaxis as revealed by a rapid and drastic drop in core body temperature (T_{core}) following systemic administration of allergen(8) (Fig.1A). When we examined various tissues in these anaphylactic WT mice, as expected, we observed widespread and vigorous MC degranulation (Fig.1B). The conventional role of MCs in anaphylaxis is their actions on blood vessels, specifically vasodilation and vascular leakage, which in principle, can cause hypothermia during anaphylaxis. Interestingly, an observation in these mice indicative of a possible role for neuronal regulation was that WT mice undergoing

anaphylaxis exhibited an “extended posture behavior” (Fig.1C) reminiscent of mouse behavior following exposure to heat challenge (e.g. 43˚C) (Fig.1C) which is a known mouse central nervous system (CNS)-controlled behavior(13).

To probe for neural underpinnings of IgE-mediated anaphylaxis, in particular those associated with hypothermia, we used a chemogenetic approach to selectively activate anaphylaxis-associated neural circuits. For this, we directed the expression of a commonly-used chemically-activated receptor Gq-DREADD (Gq-coupled Designer Receptor Exclusively Activated by Designer Drug) to neurons that are activated during anaphylaxis. This Gq-DREADD can be activated specifically by clozapine (CLZ), a clinically-used atypical antipsychotic that readily passes the blood-brain-barrier(14, 15). We reasoned that specific activation of the DREADD would evoke hypothermia, verifying the neuronal modulation of hypothermia during anaphylaxis. As shown in Fig.1D, we employed mice harboring a tamoxifen-inducible Cre recombinase driven by *Fos* ($Fos^{2A\text{-}iCreERT2}$, TRAP2(16)) with an allele of the Gq-DREADD-mCherry that is expressed in a Cre-dependent manner (RC::L-hM3Dq(17)), referred to hereafter as TRAP2-Gq mice. We first administered 4-hydroxytamoxifen (4-OHT) to TRAP2-Gq mice undergoing anaphylaxis, expecting anaphylaxis (AN)-activated neurons will express iCre-ERT2 following c-Fos, which will then recombine the RC::L-hM3Dq allele (this activity is referred to as “TRAPing” hereafter(18)), leading to a switch of the flip-excision (FLEx) structure and causing replacement of widespread eGFP expression by somatodendritic Gq-DREADD-mCherry expression in activated neurons.

To investigate if activation of these Gq-DREADD–expressing neurons is sufficient to trigger hypothermia as seen in anaphylaxis, we intravenously injected CLZ into these mice (AN_4-OHT + CLZ) on Day 8. As controls for this study, we employed (i) the same TRAPed mice but this time challenged with PBS (AN_4-OHT + PBS), (ii) non-TRAPed mice that have experienced anaphylaxis and then exposed to CLZ (AN_Corn oil +CLZ), and (iii) sham-TRAPed mice exposed to saline instead of IgE but which was still exposed to CLZ (Saline_4-OHT + CLZ). Compared to the three control groups, the AN_4-OHT + CLZ group of mice exhibited robust hypothermia, with a significantly lower temperature than all three control groups (Fig.1E), indicating that reactivation of the Gq-DREADD-expressing neurons, which were activated during anaphylaxis, results in hypothermia. Although there was hypothermia in the AN_Corn oil + CLZ group, this was not significantly different compared to the other CLZ control (Saline_4-OHT + CLZ). Taken together, these observations suggest that CNS neurons regulate hypothermia during anaphylaxis. Interestingly, the hypothermia in these mice was not of the same magnitude seen in IgE-mediated anaphylaxis (−3°C vs −6°C). This is presumably because in the latter case, in addition to the neuronal involvement, activated MCs can directly impact the vasculature causing vascular dilation and leakage which together also contribute to hypothermia.

The activation of warm thermoregulatory circuit during anaphylaxis

Next, we sought to confirm the involvement of the thermoregulatory circuit during IgE-mediated anaphylaxis by seeking indications of neuronal activation. Recent studies of

thermoregulatory neural circuits have revealed that peripheral warm and cold thermal cues are transmitted to the POA directly rostral to the hypothalamus via two distinct routes through the LPB (Fig.1F). Namely, for warm signals, the dorsal subnucleus of the LPB (LPBd) is involved, and for cold signals, the external lateral subnucleus of the LPB (LPBel) is implicated(19). Since IgE-mediated anaphylaxis is associated with hypothermia, we reasoned it would activate warm signals that are transmitted via LPBd neurons(19) to evoke hypothermic responses in mice. When we examined neuronal activation in the LPBd of mice, using c-Fos staining(20), we found markedly more activated neurons in the LPBd of WT mice that had experienced anaphylaxis compared to the vehicle control, or to $Kit^{W\text{-}sh/W\text{-}sh}$ mice (MC-deficient mice, hereafter referred to as Wsh) undergoing anaphylaxis (Fig.1G). This activation was also observed in the median preoptic area (MnPO; part of the POA), which receives afferent input from the LPB(12), and only in the anaphylactic group of mice (Fig.S1B). It is noteworthy that activation of some cells in the cold signal relaying LPBel was also observed in the anaphylactic group of mice. This is not unexpected as the anaphylaxis-associated sharp drop in T_{core} should evoke a corresponding cold signal that perhaps promotes the later recovery phase of anaphylaxis-associated hypothermia seen around 30 min post challenge (Fig.1A). Taken together, we found that, upon IgE-mediated MC activation, a specific thermoregulatory neural circuit is activated by a non-thermal signal from MCs, resulting in a robust, transient hypothermic response in mice, which is a key element of the anaphylactic response.

Since it has been shown that LPBdPOA activation in mice elicits hypothermic responses by attenuating brown adipose tissue (BAT) thermogenesis and promoting vasodilation in the skin (e.g., tail) (13, 21), we next examined these specific body sites for thermal changes during anaphylaxis, specifically, decreased BAT temperature (T_{BAT}) and increased tail temperature (T_{tail}) which is a reflection of vasodilation in the tail (21). These thermal changes can be measured by infrared imaging of the BAT region (interscapular region, in the back of the neck) and the tail(21). Compared to the vehicle control, anaphylactic mice experienced marked inhibition of BAT thermogenesis, which preceded the drop in T_{core} (Fig.1H-J) indicating that BAT was driving this thermal change. Surprisingly, we did not observe any increase in T_{tail} of anaphylactic mice compared to vehicle control (Fig.S1C). When we examined the back skin of mice as another site for skin vessel dilation, we observed a marked drop in temperature, but this appeared to be the result of the drop in T_{core} as the latter preceded the drop in back skin temperature (T_{back}) (Fig. S1D and E). Presumably, the drop in T_{core} during anaphylaxis is primarily due to a marked drop in BAT thermogenesis. Thus, during anaphylaxis, MC projection to the CNS contributes to hypothermia by activating a peripherally warm thermoregulatory neural circuit with ascending hubs in the LPBd and the MnPO. These thermoregulatory sites in the brain initiate the attenuation of BAT thermogenesis, which contributes to the marked lowering of T_{core}.

TRPV1$^+$ sensory neurons promote hypothermia during anaphylaxis

We next sought to demonstrate that the peripheral neural afferents (thermosensory neurons) provide key input to the anaphylaxis-hypothermia neural circuit we have hitherto defined. For this purpose, we isolated DRGs, one of the sites where the major population of

thermosensory neurons reside, to assay for phosphorylated ERK (p-ERK), a well-established indicator of sensory neuron activation(22). We found markedly more p-ERK in the DRGs of WT mice undergoing anaphylaxis than in either Wsh mice exposed to IgE/allergen or vehicle control mice (Fig.2A), indicating that these sensory neurons are activated during anaphylaxis in a MC-dependent manner.

We then asked which specific peripheral sensory neurons relay the anaphylaxis-associated biochemical cues from MCs. Using a candidate gene approach, we focused on *Trpv1* and *Trpv4*, which both encode ion channels responsive to thermal cues in the physiologic range (TRPV4) or slightly hyperthermic range (TRPV1)(11). However, the latter is also known to be activated within the physiologic range via Gq→PKC-mediated phosphorylation(23). We found that *Trpv4*$^{-/-}$ mice exhibited a T_{core} drop following IgE-mediated anaphylaxis that was not significantly different from that of WT mice (Fig.2B). Regarding *Trpv1*, we found that *Trpv1*$^{-/-}$ mice exhibited a significantly attenuated T_{core} drop compared to WT mice (Fig.2B), suggesting TRPV1 possibly functions as a peripheral thermosensor responding to anaphylaxis-associated chemical signals from MCs. That this response is attenuated but not eliminated in *Trpv1*$^{-/-}$ mice could be rooted in multiple (mutually non-exclusive) factors, such as other key contributory thermal-sensing neural afferents, compensatory overexpression of other thermosensors in *Trpv1*$^{-/-}$ mice, and modulatory effects of non-neural cells on the anaphylaxis-hypothermia pathophysiology, such as heat dissipation caused by vascular changes induced by IgE/allergen-activated MCs.

Since TRPV1 is expressed not only in primary sensory neurons but also in non-neural cells(24–26), we selectively rescued the *Trpv1* gene in the sensory neurons of *Trpv1*$^{-/-}$ mice by specifically directing the expression of *Trpv1-eGFP* to these neurons via adeno-associated viruses (AAVs). We intended to record if this sensory neuron-specific rescue of TRPV1 expression could restore the hypothermia response in allergen-challenged mice. For this study, as illustrated in Fig.2C, we designed an AAV expressing the *Trpv1-eGFP* fusion gene under a neuronal specific promoter, hSyn(27), in a serotype that preferentially transduces peripheral neurons(28), referred to as AAV-PHP.s-hSyn-Trpv1-eGFP. For controls, we also generated a similar AAV under the same promoter but expressing only *eGFP*, AAV-PHP.s-hSyn-eGFP. Approximately 5×10^{11} viral genomes (vg) of each of these viral particles were administered intravenously to *Trpv1*$^{-/-}$ mice as described previously(28). The administration of AAV-PHP.s-hSyn-Trpv1 in the *Trpv1*$^{-/-}$ mice resulted in TRPV1 expression in 12% of their DRG neurons (Fig.S2A). Four weeks later, allowing sufficient time for the *Trpv1*$^{-/-}$ mice to express either the *Trpv1-eGFP* rescue transgene, or *eGFP* control, we compared the hypothermic response to IgE/allergen challenge. We observed that the *Trpv1*-rescued mice experienced a robust and significantly deeper T_{core} drop vs *eGFP*-mice (Fig.2D). However, a hypothermic response of the latter mice of > 4˚C (vs >8˚C in *Trpv1*-rescued) indicates other molecular pathways contribute. Thus, our sensory neuron-specific rescue experiments unambiguously implicate TRPV1^{+} sensory neurons as key peripheral feeders in the anaphylaxis-hypothermia neural circuit. In view of robust previous evidence on TRPV1, these peripheral neurons are thermo-nociceptors for physiologic functioning, yet our data do not exclude other molecular contributory mechanisms in anaphylaxis-hypothermia.

Chemogenetic activation of TRPV1$^+$ sensory neurons triggers anaphylactic-like responses

Based on these results, namely the implication that TRPV1$^+$ sensory neurons are peripheral sensory transducers of anaphylaxis-hypothermia, we next sought to investigate if chemogenetically activating TRPV1$^+$ sensory neurons suffices to induce responses seen in anaphylactic mice, even in the absence of MCs. For this, we again employed the chemogenetic Gq-DREADD tool which allowed us to selectively activate TRPV1$^+$ sensory neurons, yet without activating MCs. We crossed TRPV1-Cre mice with Gq-DREADD-FLEx mice to generate TRPV1-Gq-DREADD transgenic mice (Fig.2E) which allowed us to selectively activate TRPV1-expressing cells in a Gq-PLC/cAMP pathway-dependent manner, by administration of the specific ligand for Gq-DREADD, clozapine N-oxide (CNO)(29). Notably, certain MC products such as histamine and tryptase can activate or sensitize TRPV1 receptor via Gq signaling, either through Gq-PLC-PKC or Gq-cAMP-PKA pathways(30, 31). Therefore, using this Gq-DREADD approach, we could better recapitulate the activation of TRPV1$^+$ sensory neurons during anaphylaxis and probe the sufficiency of this activation for inducing anaphylactic-like hypothermia. Though other cell types have been reported to express low levels of TRPV1, which suggests that they might also be activated by CNO, we believe the anticipated hypothermic effect will be mainly due to TRPV1$^+$ sensory neurons since *Trpv1* is abundantly expressed in sensory neurons compared to other cell types.

We found that upon CNO administration, hypothermia followed as evidenced by the sharp drop in T_{core}, which was also accompanied by a decrease in BAT thermogenesis (Fig.2F-G). With the control group of RC:L-hM3Dq mice administered with CNO, we confirmed that these effects were not due to any potential effect of CNO in driving hypothermia. Unlike anaphylaxis, where tail-associated heat dissipation was not observed, we observed an initial spike at t=3min (*albeit* it is globally not significant) as shown in Fig.S2B, which is another typical response when the thermoregulatory neural circuit is activated. When we assayed for neuronal activation in the LPBd region in the brain stem, which is upstream of the BAT activity, we observed activation of LPBd neurons (Fig.2H) confirming that specific activation of TRPV1$^+$ sensory neurons can activate hubs in the brain involved in thermoregulation. Additionally, the CNO-administered TRPV1-DREADD mice also exhibited the characteristic extended posture (Fig.2I) reminiscent of the behavior of mice experiencing anaphylaxis-hypothermia or receiving a heat signal (Fig.1C). We found that another prominent outcome of IgE-mediated anaphylaxis in mice is a drastic drop in blood pressure (Fig.S2C). Interestingly, we found that the activation of TRPV1$^+$ sensory neurons can also induce a marked blood pressure drop in the mice (Fig.2J). Thus, stimulation of peripherally innervated TRPV1$^+$ sensory neurons can lead to activation of the neuronal network involved in thermoregulation and seemingly also neuronal networks involved in regulating blood pressure.

Since capsaicin is a well-known natural agonist for TRPV1, we also examined its capacity to induce hypothermia. We found that intraperitoneal administration of capsaicin evoked in WT mice a similar hypothermic response as CNO in the TRPV1-DREADD mice (Fig.S2D-H), indicating that systemic activation of TRPV1$^+$ sensory neuron with a naturally occurring highly specific activator is sufficient to induce a sharp drop in T_{core} which is preceded

by inhibition of BAT thermogenesis, as well as a drop in blood pressure. Since MCs are not activated by capsaicin(32), the capsaicin effect is also MC-independent. Therefore, both mechanisms, chemogenetic activation of TRPV1$^+$ cells and direct capsaicin-mediated activation of TRPV1, can trigger anaphylaxis-like responses in mice.

MCs activate TRPV1$^+$ sensory neurons via their granules

Having established that activation of TRPV1$^+$ sensory neurons in the periphery is sufficient to trigger hypothermia in WT mice, we sought to investigate if MCs and their products are responsible for directly activating these sensory neurons. For this, we conducted an ex vivo live-imaging experiment using freshly isolated TG tissue from Advillin-GCaMP6 mice. GCaMP6 is a genetically encoded calcium indicator (GECI), which enabled us to identify cell activation indicated by calcium influx, and the transgene is driven by the sensory neuron-specific advillin promoter. Isolated TGs were co-incubated with adherent IgE-sensitized RBL-2H3 MCs (a rat MC line) in a culture dish (Fig.3A). Thereafter, the MCs were selectively induced to degranulate and release granules by adding TNP-OVA. Using a fluorescent microscope, we then measured calcium dynamics of the TG neurons over time. We observed a significant calcium response following MC degranulation compared to the baseline (Fig. 3B-C), indicating that MC activation evokes activation of sensory neurons. When we subsequently exposed the same TGs to capsaicin, we found that some MC-activated neurons also responded to capsaicin, indicating their TRPV1$^+$ lineage.

We next sought to investigate the mechanism of how MCs activated TRPV1$^+$ sensory neurons. We noticed from microscopy of the mouse tissues (ear pinna and trachea) that a significant number of MC granules had deposited on nerve fibers (Fig.3D and Fig.S3A), suggesting physical contact between recently released MC granules and sensory neurons in the perivascular space as the mode of activation. Scanning electron microscopy (SEM) of the ear pinna of anaphylactic mice appeared to reveal several MC granules adhering to the surface of a single nerve fiber (Fig.3E). These observations drove us to hypothesize that MC can directly activate TRPV1$^+$ sensory neurons via their granules. To test this hypothesis, we investigated if cultured DRG neurons can be activated by isolated MC granules. For this study, we isolated MC granules from IgE/allergen-activated RBL-2H3 cells and then exposed them to isolated DRG neurons from Advillin-GCaMP6 mice. We observed an appreciable calcium influx in DRGs when treated with isolated granules (Fig.3F). A significant portion of these responding DRG neurons subsequently responded to capsaicin, indicating their TRPV1$^+$ lineage. In summary, these observations suggest that following activation of tissue MCs, exocytosed granules deposit on neighboring sensory neurons, and this event can result in the activation of TRPV1$^+$ sensory neurons.

MC granule-derived chymase activates TRPV1$^+$ sensory neurons

Several MC mediators found in exteriorized granules are known to activate neurons, including histamine, serotonin, as well as a protease, tryptase(33). Chymase is another prominent MC protease released during IgE-mediated anaphylaxis but its role remains unknown despite its potential in serving as a biomarker for anaphylaxis in clinical settings(34, 35). In view of its significant abundance in the circulation of anaphylactic subjects, we investigated if chymase could contribute to anaphylaxis by activating TRPV1$^+$

sensory neurons. First, we compared IgE-mediated anaphylaxis in WT and *Mcpt4*$^{-/-}$ mice, a mutant mouse strain deficient in chymase production(36). We found that the T_{core} drop in *Mcpt4*$^{-/-}$ mice was significantly attenuated compared to WT mice (Fig.4A) implicating chymase in anaphylaxis-hypothermia. In support of this deduction, WT mice treated with antagonists against the chymase receptor PAR1 (37) also experienced an attenuated anaphylactic hypothermia (Fig.4B), pointing to MC-derived chymase as a major contributor to the hypothermic response during anaphylaxis.

If chymase is activating TRPV1^{+} sensory neurons, we reasoned that these neurons should express its complementary receptor, PAR1, which is encoded by the gene *F2r*(38). Therefore, we surveyed for the expression of this gene in TRPV1^{+} sensory neurons in publicly available gene expression profiles of DRG cells from the Gene Expression Omnibus (https://www.ncbi.nlm.nih.gov/geo/) and the Mouse Brain Atlas (http://mousebrain.org/). One bulk RNA-seq dataset from mice that we analyzed (produced by Zheng et al.(39)) revealed that TRPV1^{+} sensory neurons, especially peptidergic type 1 and 2 neurons, express high levels of *F2r* (Fig. 4C). Additionally, single-cell RNA-seq data of DRG neurons from mice generated by multiple groups were analyzed, where cell type clusters were predefined. From these analyses, one representative dataset is shown in Fig. 4D (Zeisel et al.(40)), from which we also detected high-level expression of *F2r* in TRPV1^{+} sensory neurons, mainly peptidergic neurons, with the double-positive cell percentage of each cluster plotted in Fig.4E. These findings from mice were also observed in datasets obtained from rhesus macaques by Kupari et al.(41) (Fig.S4A-B), suggesting PAR1 expression by TRPV1^{+} sensory neurons is evolutionarily conserved from rodent to primate. That *F2r* is amply expressed on DRG neurons of mice was confirmed by RNAscope specific probing for *F2r* (Fig.4F). Overlapping expression of *F2r* and *Trpv1* was also confirmed by this assay (Fig.4F).

To investigate if chymase can directly activate TRPV1^{+} sensory neurons, we measured calcium influx in isolated DRG neurons expressing GCaMP6 following exposure to recombinant chymase. We found that 20 ng/ml of recombinant chymase (serum or plasma chymase levels during anaphylaxis are about 25 ng/ml in mice (42) and 90 ng/ml in human patients(35)) evoked a substantial calcium response in DRG neurons, a significant percentage of which also responded to capsaicin, indicating their TRPV1^{+} lineage (Fig.5A). We then repeated this experiment in DRG neurons isolated from *Trpv1*$^{-/-}$ mice (injected with AAV9-GCaMP6 intrathecally so that DRG neurons express GCaMP6) (Fig.5B, left). We found that chymase could not induce an increase of calcium influx in *Trpv1*$^{-/-}$ sensory neurons (Fig.5B, right), suggesting TRPV1 expression as a necessary prerequisite for DRG neurons' response to chymase. To examine the impact of chymase on neuronal excitability of primary sensory neurons, we recorded action potentials of cultured DRG neurons in response to recombinant chymase. We also found that recombinant chymase increased the number of action potentials in DRG neurons isolated from WT mice (Fig.5C). This effect was not detectable in DRG neurons isolated from *Trpv1*$^{-/-}$ mice (Fig.5D). These patch-clamp data extend our calcium imaging finding and suggest that chymase can activate and increase excitability of DRG sensory neurons, a process dependent on the *Trpv1* gene, possibly indicating a key role for TRPV1 ion channels involved in the sensory neuronal activation response to chymase.

Since both isolated MC granules and chymase can activate TRPV1$^+$ sensory neurons directly, we sought to assess the importance of chymase compared to other components of isolated MC granules in activating neurons. For this, we examined how much of the neuronal calcium response was inhibitable by TY-51469, a potent chymase inhibitor derived from benzothiophenesulfonamide(43). As shown in Fig.5E, the chymase inhibitor appeared to have an overwhelming effect in suppressing TRPV1$^+$ sensory neuronal response to MC granules, suggesting that the calcium flux evoked by isolated MC granules shown earlier in Fig.3F was largely due to chymase.

Proteases are believed to activate targeted cells through actions on PARs which initiate a sequence of intracellular reactions(44). To test if the cognate receptor for chymase, PAR1, is responsible for the response of these neurons, we examined the calcium response of DRG neurons to chymase using selective PAR1 antagonists, SCH 79797 or RWJ 56110. As shown in Fig.5F and Fig.S5A, the chymase-mediated activation of the TRPV1$^+$ sensory neurons was blocked by PAR1 antagonists. Since chymase can activate PAR2 receptors which are also expressed on TRPV1 sensory neurons(44), we examined chymase-induced calcium responses in TRPV1$^+$ sensory neurons to see they could be blocked by a potent PAR2 antagonist, FSLLRY-NH2. We found that the PAR2 antagonist was only minimally able to suppress neuronal responses to chymase (Fig.5G). Therefore, chymase activates TRPV1$^+$ sensory neurons primarily through its cognate receptor, PAR1.

As the transcriptomic data suggested that PAR1 and TRPV1 receptors are co-expressed by a significant population of peptidergic neurons, we next tested if chymase could induce the release of neuropeptides, which is one of the key features when these peptidergic neurons are activated(45). We found that chymase by itself did not promote the release of neuropeptide (Fig.S5E), however, it could sensitize DRG neurons and promote CGRP release to histamine (Fig.S5B-D).

In ensemble, we have shown that MC chymase can directly activate primary sensory neurons via PAR1 which then activates TRPV1 to mediate calcium influx and facilitate depolarization.

Discussion

In mice, we have discovered an element of the body's thermoregulatory neural machinery which underlies the profoundly hypothermic response to IgE-mediated anaphylaxis as summarized in Fig.6. These findings thus describe a hitherto overlooked functional link between two primal evolutionary defense mechanisms, namely thermal homeostasis and innate immunity. The neural circuit we implicate has peripheral afferents of TRPV1$^+$ sensory neurons, which transmit via the brainstem thermoregulatory nucleus LPBd to the pre-hypothalamic POA. The POA is the epicenter of thermoregulation and drives thermoregulation by activating or attenuating BAT thermogenesis as one of the mechanisms. Indeed, the >8˚C hypothermia in response to massive MC degranulation was driven partially by diminished BAT thermogenesis. While we did not observe vasodilation in the skin as a mechanism for heat dissipation, we cannot rule out the possibility that the infrared imaging

we utilized to assess vasodilation may be compromised by MC-mediated vascular leakage that is occurring concurrently(46, 47).

Our findings suggest a concept of biochemical activation of a neural thermoregulatory organization with peripheral sensor and central effector mechanisms subserving hypothermia. In other words, anaphylaxis-induced chemical signals activate peripheral thermal-sensing neurons in the absence of a thermal cue, resulting in profound hypothermia. This could be referred to as an anaphylaxis-pseudo-heat signal, which is transmitted by the peripheral TRPV1$^+$ sensory neurons. The cellular source for this pseudo-heat signal is nearby MCs, which release prestored granules upon activation by IgE/allergen, and some of the exteriorized granules readily deposit on nerve fibers. The resulting physical interaction potentially exposes receptors on neurons to concentrated amounts of MC products presented on particles. When ligands are immobilized on particles, they evoke a more potent signal than in solution as they are more effective in crosslinking complementary receptors on the cell surfaces(48). Although several MC products reportedly can activate sensory neurons(33), we found that chymase, a protease and a major component of MC granules, specifically activated TRPV1$^+$ sensory neurons as DRG neurons from *Trpv1*$^{-/-}$ mice responded poorly to chymase. The importance of MC-derived chymase in anaphylaxis could be deduced from the observation that chymase-deficient mice or WT mice pretreated with chymase receptor antagonists exhibited attenuated anaphylactic responses. Additionally, antagonists of the chymase receptor were shown to suppress much of the calcium responses of TRPV1$^+$ neurons to MC granules, implying that chymase is the major activator of TRPV1$^+$ neurons found in MC granules. A caveat, however, is that during isolation of MC granules some of their soluble cargo may have been released and so may not be present in isolated granules. Therefore, we cannot yet exclude possible roles of other MC products especially soluble mediators such as histamine and serotonin, which have both been shown to activate the TRPV1 receptor(33).

PAR1-PAR4 are a subfamily of G-protein-coupled receptors whose activation mechanism is conserved(49). Typically, PARs become activated when their extracellular amino terminus is cleaved by their own ligand protease(s). This activation triggers the intracellular signaling pathway via Gq proteins, and this is also true in TRPV1$^+$ neurons as treatment with a PAR2 ligand (such as tryptase) was shown to phosphorylate TRPV1 through PKC, which is downstream of the Gq-PLC cascade(44). We have found co-expression of TRPV1 and PAR1 mRNAs by peptidergic neurons not only in mice but in higher mammals such as rhesus macaques. In vitro findings that antagonists for PAR1 blocked chymase-mediated activation of TRPV1$^+$ sensory neurons suggested chymase activated TRPV1 through PAR1, presumably through the same Gq-PLC-PKC signaling pathway as seen with PAR2 activation. Taken altogether, these findings point to a critical role for MC chymase and its interaction with TRPV1$^+$ sensory neurons through its cognate receptor PAR1 in IgE-mediated anaphylaxis. Of course, future studies in PAR1 null mice or mice deficient in PAR1 expression exclusively in TRPV1$^+$ sensory neurons are required to further confirm the role of chymase-PAR1 on these nociceptors.

Although our studies revealed the previously unappreciated contribution of the nervous system to anaphylaxis, our observations, in a way, also echoed the historical view of

MC-mediated vascular changes driving anaphylaxis. Indeed, this was supported by the evidence that the T_{core} drop in the AN-TRAPed-CLZ mice and in *Trpv1*$^{-/-}$ mice were modest compared to anaphylactic WT mice, emphasizing the concurrent contributions of MC-mediated vasodilation and vascular leakage to hypothermia. Additionally, one might argue that in additional to periphery sensors, the POA also plays an important role in detecting temperature changes, especially internal cues, as neurons located in POA can directly sense blood temperature and respond accordingly(11). Future studies will elucidate if MC products that diffuse into blood can directly activate neurons in the POA and thereby trigger a hypothermic response. It will also interesting in the future to examine and distinguish the roles of TRPV1^{+} neurons from different ganglia (DRG/TGs versus nodose/jugular) in the context of anaphylaxis, as they innervate different organs and tissues.

In view of the seemingly detrimental role played by the peripheral MC-TRPV1 sensory neuron interaction during IgE-mediated anaphylaxis, why does this axis even exist? Presumably, the close physical proximity between MC and nerve fibers and their associated interactions evolved to rapidly respond to a local cutaneous challenge by microbes and allergens, including injected insect venom. Upon activation of perivascular MCs by these extrinsic agents, exteriorized MC mediators will activate TRPV1^{+} sensory neurons, which release neuropeptides such as CGRP that, together with MC mediators, will promote local vasodilation and vascular leakage(33, 50, 51). These vascular events could be beneficial to the host by slowing down or reducing the systemic spread of the foreign agents and facilitating their neutralization and clearance by promoting seepage of circulating humoral factors (such as complement and immunoglobulins) and extravasation of phagocytic cells(6, 52). Concurrently, activated TRPV1^{+} sensory neurons can potentially trigger pain and itch responses to promote scratch-mediated microbe and insect removal. However, when the microbe/allergen exposure is systemic, as is the case during IgE-mediated anaphylaxis, MC activation is no longer a local phenomenon. Instead, MC activation likely occurs simultaneously throughout the body, resulting in the widespread activation of peripheral TRPV1^{+} sensory neurons. The intensity and magnitude of this activation could potentially surpass the threshold for activating the thermoregulatory circuit downstream of TRPV1^{+} sensory neuron. Presumably, the threshold to trigger the abrogation of BAT thermogenesis is not attained when local MCs and TRPV1 neuronal activation occur. Thus, the systemic activation of the thermoregulatory circuit during anaphylaxis could be an unintended consequence of widespread hyperactivation of the MC-TRPV1 neuronal axis.

Whereas anaphylaxis in rodents is measured by assessing hypothermia(8, 53), anaphylaxis in humans is primarily assessed by measuring hypotension(54). Although hypothermia is not routinely assessed in humans during anaphylaxis, it does not mean that intense temperature regulation does not occur. Indeed, it has been reported that humans experiencing anaphylaxis have damp skin, which is due to sweating, an alternate mechanism employed by humans to regulate body temperature(55). Since sweating is a major mechanism for heat loss in humans but is absent in rodents, the major effector organs responding to thermal challenges in rodents and man appear different. Indeed, even though BAT has been implicated recently in thermogenesis in humans(56) its role may not be as important as in rodents. Nevertheless, initiating the peripheral TRPV1^{+} sensory neuron pathway leading to activation of the CNS could be conserved as clinical studies have revealed that both

TRPV1 agonists and antagonists may regulate the temperature in humans(57, 58). Even though our studies of anaphylaxis in mice were mostly focused on thermoregulation, it is conceivable that the neuronal circuit regulating blood pressure may be involved in a similar manner in both animals and humans. This is especially the case considering how fast the nervous system downregulates blood pressure following the specific activation of baroreceptors in blood vessels(59–61). Indeed, our data have revealed that activation of $TRPV1^+$ sensory neurons can concurrently induce a blood pressure drop in mice, suggesting that during anaphylaxis, the MC-$TRPV1^+$ sensory neurons axis also transmit signals to the blood pressure regulation center in the brain. Other evidence of this comes from the finding that capsaicin consumption or administration reduces blood pressure(62). Thus, during anaphylaxis, both thermoregulatory and blood pressure regulatory centers in the CNS may be simultaneously triggered by peripheral $TRPV1^+$ sensory neurons through the actions of perivascular MCs. As there exists a dire need for effective ways to prevent this life-threatening disorder, our finding of the role of a MC-sensory neuron-CNS axis in driving anaphylactic responses provides valuable insights that may lead to new therapeutic options.

Materials and Methods

Mouse strains

All procedures related to mice were performed in strict accordance with the animal protocol approved by the of Duke University Institutional Animal Care and Use Committee. Seven- to 12-week-old female and male mice were used for most of these studies. The *Mcpt4*$^{-/-}$ mouse strain was a gift from Dr. Magnus Abrink at Swedish University for Agricultural Sciences, Uppsala, Sweden. The Mcpt5-Cre strain was a gift from Dr. Axel Roers, University of Technology, Dresden, Germany. The rest of the strains were obtained from Jackson Laboratories (see list in Table S1).

Cell culture

RBL-2H3 cells were cultured in minimum essential medium containing 15% FBS and 1% Anti-Anti. For mouse DRG cultures, DRGs were aseptically isolated from mice and digested with collagenase (1.25 mg/ml)/dispase-II (2.4 units/ml) at 37°C in a humidified 5% CO_2 incubator for 60 min. Flame-polished Pasteur pipettes were used to mechanically agitate the ganglia. Dissociated DRG cells, after filtration through 70 μm nylon cell strainers, were plated on poly-D-lysine- and laminin-precoated cover slips and grown in a Neurobasal Medium, supplemented with 10% FBS, 2% B27 supplement, and 1% Anti-Anti. All cells were cultured at 37°C in a humidified water-jacketed incubator under a 5% CO_2–95% air atmosphere.

MC depletion in Mcpt5-iDTR mice

MCs in Mcpt5-$Cre^{+/-}$-iDTR mice were conditionally depleted as follows: 7-week-old Mcpt5-$Cre^{+/-}$-iDTR mice and Mcpt5-$Cre^{-/-}$-iDTR littermates were given five intravenous injections of 200 ng of DT per mouse for five consecutive days.

Anaphylaxis

To elicit anaphylaxis, mice were first sensitized with TNP-specific IgE (10 μg in saline) by intravenous injection. After 18 hours, mice were injected intravenously with TNP-OVA. For temperature monitoring, 1 μg TNP-OVA was injected. For brain c-Fos immunostaining and TRAPing, 1.2 μg TNP-OVA was injected two hours before mice were euthanized. For DRG p-ERK immunostaining, whole mount tissue staining and SEM, 2 μg TNP-OVA was injected 10 min before mice were euthanized. For anaphylaxis in MC-depleted mice, 3 μg TNP-OVA was used. As for PAR1 antagonist treatment, we pretreated IgE-sensitized mice with the combination of PAR1 antagonists RWJ 56610 (0.2 mg/kg) and SCH 79797 (0.5 mg/kg) intraperitoneally 1h prior to TNP-OVA.

TRAPing

TRAP2-Gq mice were sensitized with either saline or IgE on Day 0 and then challenged with TNP-OVA on Day 1. Then each mouse received a total of 100 mg/kg of 4-OHT for TRAPing (or corn oil as a vehicle control) over a two-hour interval after induction of anaphylaxis (t=0 and 2h). 4-OHT was prepared as previously described(16).To activate TRAPed neurons, mice were injected intravenously with 0.1 mg/kg CLZ or PBS on Day 8.

T_{BAT}, T_{tail}, T_{back}, and T_{core} measurements

T_{core} was measured with a rectal microprobe thermometer at the specified time points, while T_{BAT}, T_{tail}, T_{back} were measured using a thermal infrared camera (FLIR C5) with a protocol modified/combined based on previous studies (21, 63, 64). Briefly, for T_{BAT}, the interscapular region of mice was shaved one day before measurement; for T_{back}, the back below the interscapular region was shaved one day before measurement. Snapshot images were taken at the specified time points, which were later analyzed with FLIR Thermo Studio software. The highest temperature in the interscapular region or the back skin (excluding the interscapular region) was taken as the T_{BAT} *or* T_{back}, respectively. T_{tail} was taken as the average of a 5 mm-line of tail at the region that is 1 cm from the base of the tail.

Blood pressure measurement

The mean arterial blood pressure (MAP) was measured through the right femoral artery of mice as described previously(65). Briefly, mice were placed into the induction chamber and anesthetized with 5% isoflurane in 30% oxygen balanced with nitrogen, then placed in the supine position and maintained in 1.5% isoflurane via face mask. A 1-cm skin incision was made in the right groin to expose the femoral artery and vein, which were cannulated with PE-10 tubing for arterial blood pressure and drug administration (for the IgE-sensitized WT mice but not for the TRPV1-DREADD mice and capsaicin administered WT mice). Heparin (1:10, 50 μL, 5 U) was given through the arterial line. MAP was measured through a digital blood pressure transducer connected to a Bridge Amp (ADInstruments, Dunedin, New Zealand). ECG needle probes were placed in both forearms and the left hind limb. The ECG was recorded via Animal Bio Amp (ADInstruments). Rectal temperature (monitored with a mouse rectal temperature probe) was monitored and heat lamp and heating pad were supplied to keep the temperature at 37.0±0.2°C. Baseline recording was started when their core body temperature recovered to 37°C after the surgery. Then 5 min later, mice

were treated with different stimuli: IgE-sensitized WT mice received 1μg TNP-OVA in 100 μl PBS through the femoral vein cannulation, TRPV1-DREADD or the control strain RC::L-hM3Dq mice received 2 mg/kg CNO in 200 μl PBS through intraperitoneal injection, and 100 μg capsaicin was administered intraperitoneally into WT mice.

Virus injection

For the *Trpv1* rescue experiment, we used AAV-PHP.s-hSYN1-TRPV1 and AAV-PHP.s-hSYN1-eGFP produced by the Duke Viral Vector Core. Eight-week-old $Trpv1^{-/-}$ mice were injected intravenously with ~45×10^{10} vg AAVs. Four weeks later, passive systemic anaphylaxis (PSA) was elicited in the mice. Body, BAT and tail temperatures were monitored. For the $Trpv1^{-/-}$ DRG calcium imaging experiment, ~41×10^{10} vg AAV9-GCaMP6 was injected intrathecally into 8-week-old $Trpv1^{-/-}$ mice. Four weeks later, DRGs were isolated from these mice for calcium imaging.

Systemic TRPV1 activation experiments

TRPV1-DREADD—To generate TRPV1-DREADD mice, TRPV1-Cre mice were crossed with Gq-DREADD-FLEx mice. CNO (2 mg/kg) was injected intraperitoneally into TRPV1-DREADD mice. T_{BAT}, T_{tail} and T_{core} were monitored.

Capsaicin—WT mice were injected intraperitoneally with 100 μg Capsaicin in 5% Tween-80 in PBS or vehicle control alone. T_{BAT}, T_{tail} and T_{core} were then monitored.

MC granule isolation

MC granules were isolated as described previously(66). RBL cells were cultured in 175 cm^2 flasks until 70% confluency, then cells were sensitized with 0.5 μg/ml IgE for 18 h before activating with 10 ng/ml TNP-OVA. Cells were left in the 37˚C incubator for 1 h for MCs to fully degranulate. 1 h later, the supernatant was collected and spun down at 1200 rpm for 5 min at 4˚C twice to remove cells or cell debris in the supernatant. Afterwards, a final high-speed spin at 3000 × g for 15 min was performed. An Optima L-90K ultracentrifuge (Beckman Coulter) was used for centrifugation. The collected granule pellet from one 175 cm^2 flask was resuspended in 0.5 ml of Tyrode's buffer and stored in −80˚C for later usage.

Immunostaining

Mice were perfused transcardially with PBS followed by 4% PFA in PBS.

Section staining: Brains or spines were dissected, post-fixed in 4% PFA for 12–24 h and then placed in 30% sucrose in PBS for 24–48 h at 4˚C. DRGs were isolated from spines thereafter. Brains and DRGs were then embedded in Optimum Cutting Temperature compound and stored at −80°C until sectioning. For brains, 40-μm floating sections were collected into cryopreservation solution (5:3:2 PBS: ethylene glycol: glycerin). For c-Fos immunostaining, sections were washed in PBS for three times and then incubated in 0.3% Triton X-100 in PBS (PBST) and 5% donkey serum for 2 h at room temperature (RT) and then stained with rabbit anti-Fos (1:1000) overnight at 4°C in 0.3% PBST and 5% donkey serum. All sections were washed 3 × 10 min in PBST and additionally stained with donkey anti-rabbit Cy3 (1:1000) in 0.3% PBST and 5% donkey serum for 2 h at RT and then washed

2 × 20 min in PBST, then with PBS for 2 × 20min prior to mounting onto slides and coverslipping in Fluoroshield with DAPI. For DRGs, 15-μm sections were cut and collected onto coated slides. For p-ERK staining, sections were washed in PBS to remove the OCT and then incubated in 0.3% Triton X-100 in PBS (PBST) and 5% donkey serum for 1 h at RT and then stained with rabbit anti-p-ERK (1:500) overnight at 4°C in 0.3% PBST and 5% donkey serum. All sections were washed 3 × 10 min in PBST and additionally stained with donkey anti-rabbit Cy3 in blocking buffer for 1 h at RT and then washed 3 × 10 min in PBST. Sections were then stained with Neuro-Trace Deep Red Nissl based on the manufacturer's instructions prior to being mounted in Fluoroshield with DAPI.

Whole-mount tissue staining—Ears and tracheal tracts were dissected and fixed in 4% PFA overnight at 4˚C. Then tissues were washed in 0.3% PBST for 3 × 20 min prior to being blocked in 0.3% PBST and 5% donkey serum for 2 h at RT. Then tissues were stained with rat anti-CD31 (1:200), rabbit anti-ß3 tubulin (1:500) in the blocking buffer overnight at 4˚C. All tissues were washed 3 × 20 min in PBST and additionally stained with donkey anti-rabbit Cy3, donkey anti-rat 647 (1:1000) and FITC-avidin (1:500) in blocking buffer for 1 h at RT and then washed 3 × 10 min in PBST. Then tissues were mounted with Prolonged Diamond.

In situ hybridization (ISH)

Sections of mouse DRGs were freshly prepared. In situ hybridization was performed using the RNAscope system (Advanced Cell Diagnostics) in accordance with the manufacturer's instructions, using a protocol designed for the Multiplex Fluorescent Kit v2. We used probes directed against murine *F2r* and *Trpv1*. After completion of the RNAscope protocol, the slides were incubated with Nissl/NeuroTrace-640 for 1 hour at room temperature in a humidified chamber. Sections were washed several times with PBS and mounted with a few drops of DAPI Fluoromount mounting medium.

Fluorescent image analysis

Fluorescent images were obtained with a Leica THUNDER imaging system and were analyzed with Fiji (ImageJ, NIH). For fluorescent image quantification, in general, ≥5 images of each tissue were analyzed and then the mean of these images of each tissue was obtained and graphed. For 3D modeling, the surface function of Imaris software (Bitplane) was used to reduce the non-specific signal and render 3D modeling surfaces for every channel based on the mean fluorescence intensity, to achieve the morphology of nerve fibers, MCs and blood vessels.

Scanning electron microscopy (SEM)

Ear pinnae were dissected from mice 15 min after PSA and fixed in 4% PFA overnight at 4˚C. Then ear tissues were dehydrated with an ethanol series and finally dried in hexamethyldisilane (HMDS) (Sigma, 440191). Ear samples were coated with gold for 600s employing the SPUT6 Vacuum Sputter Coater (Kurt Lesker PVD 75) before being imaged with a scanning electron microscope (FEI XL30 SEM-FEG).

Calcium imaging

Calcium imaging was conducted in mouse DRG neurons. DRG neurons were isolated from Advillin-GCaMP6 or *Trpv1*$^{-/-}$ GCaMP6 mice 18 h before a calcium imaging experiment. The imaging was performed by recording cells responding to stimuli in perfusing buffer which contained 140 mM NaCl, 10 mM D-(+)-Glucose, 1 mM $MgCl_2$, 2 mM $CaCl_2$, 5 mM KCl, 10 mM HEPES, pH = 7.4, osmolarity = 320 mOsm/L. Ca^{2+} signals were measured using green emitted light in a 3s interval. Baseline average fluorescence intensity was calculated as F_0. Fold change of signal amplitudes at each time point are presented as $\Delta F/F_0 = (F_t\text{-}F_0)/F_0$; ratio of fluorescence difference (F_t-F_0) to basal value (F_0). F_t represents the fluorescence intensity at each time point. $F_t \geq 5\%$ from baseline levels was considered a positive response to a ligand. In some studies, 40 mM KCl was added at t=22~424min to activate neurons.

Patch-clamp recording

Mouse DRG neurons were cultured as described above. After 24-hour culturing, whole-cell patch-clamp recording was performed on small-diameter DRG neurons (<50 μm) at room temperature using patch pipettes with a resistance of 2–4 MΩ. A patch-clamp configuration which switched to current clamp mode was performed to record action potentials. The action potentials were evoked by current injection steps from 0 – 650 pA with an increment of 50 pA in 1000 ms. 100 ng/ml chymase was perfused for 2 min, and action potentials were recorded before (baseline) and soon after the perfusion with chymase.

Analysis of DRG single-cell RNA-seq data

Gene expression profiles of DRG single cells in the count scale along with clustering annotations and other relevant metadata were downloaded from the Gene Expression Omnibus (https://www.ncbi.nlm.nih.gov/geo/) or the Mouse Brain Atlas (http://mousebrain.org/). Normalization and visualization were done with the SCANPY package(67). In brief, single cell counts were scaled by the total library size, multiplied by 10,000, and log2 transformed. Highly variable genes were determined by mean and dispersion and were used as the basis for downstream analysis. After rescaling, single cells were projected onto a low-dimensional space using principal component analysis (PCA). The first 50 principal components were then used as input for uniform manifold approximation and projection (UMAP)(68) and visualized in a two-dimensional space. Cell type clusters were predefined by the original studies. To facilitate interpretation of the biological signals in a unified context, we harmonized clustering labels across DRG datasets according to a cell type mapping provided by Kupari et al(41). Specifically, we converted all cell type labels to their counterparts in the Usoskin study(69), which consisted of Th, NP1/2/3, PEP1/2, TPRM8, and NF1/2/3/4. The expression levels of mouse genes *Trpv1* (*TRPV1* in rhesus) and *F2r* (*F2R* in rhesus) were visualized in the embedded two-dimensional UMAP space.

Statistical analysis

Statistical analyses were performed by using GraphPad Prism v.9 (GraphPad Software). The statistical methods used are specified in the figure captions. Briefly, for most of the

studies, one-way or two-way analysis of variance (ANOVA) was used as a global test to discern if there is any significant statistical difference among groups; Student's t-test or two-way ANOVA or Dunnett's multiple comparison test was used as a post-hoc test later if necessary. For some analyses, unpaired Student's t-test was directly used to calculate statistical significance. A p-value of <0.05 was considered statistically significant. Data are presented as the mean ± SEM.

Supplementary Material

Refer to Web version on PubMed Central for supplementary material.

Acknowledgments

We thank Dr. Jianhua Wang from Dr. Hailan Hu's lab (Zhejiang University) for suggestions on the TRAPing experiment. We thank Dr. Ping Dong from Dr. Huanghe Yang's lab and Dr. Giselle Lopez (Duke University) as well as Dr. Junli Zhao from the Ji lab for technical support with brain processing, sectioning, staining, and mapping. We thank Dr. Yong Chen for providing the *Trpv4*$^{-/-}$ mouse strain. We thank the Duke Vector Core facility for their assistance in AAVs construction and production.

Funding:

This work was funded by the NIH R01-GM144606 (to S.N.A).

Data and materials availability:

All data needed to evaluate the conclusions in the paper are available in the manuscript or the Supplementary Materials.

References and Notes:

1. Yu JE, Lin RY, The Epidemiology of Anaphylaxis, Clin. Rev. Allergy Immunol. 54:366–374 (2018). [PubMed: 26357949]
2. Campbell RL, Fernanda-Bellolio M, Knutson BD, Bellamkonda VR, Fedko MG, Nestler DM, Hess EP, Epinephrine in anaphylaxis: higher risk of cardiovascular complications and overdose after administration of intravenous bolus epinephrine compared with intramuscular epinephrine. J. Allergy Clin. Immunol. Pract. 3, 76–80 (2015). [PubMed: 25577622]
3. Sicherer SH, Simons FER, Williams PV, Bahna SL, Chipps BE, Fasano MB, Lester MR, Virant FS, Welch MJ, Kelso JM, Mahr TA, Ownby D, Rachelefsky GS, Burrowes D, Self-injectable epinephrine for first-aid management of anaphylaxis. Pediatrics. 119, 638–646 (2007). [PubMed: 17332221]
4. Finkelman FD, Anaphylaxis: Lessons from mouse models. J. Allergy Clin. Immunol. 120, 506–515 (2007). [PubMed: 17765751]
5. Lieberman P, Garvey LH, Mast Cells and Anaphylaxis. Curr. Allergy Asthma Reports 2016 163. 16, 1–7 (2016).
6. Kunder CA, John A. L. St, Abraham SN, Mast cell modulation of the vascular and lymphatic endothelium. Blood. 118 (2011), pp. 5383–5393. [PubMed: 21908429]
7. Kemp SF, Lockey RF, Anaphylaxis: A review of causes and mechanisms. J. Allergy Clin. Immunol. 110, 341–348 (2002). [PubMed: 12209078]
8. Choi HW, Suwanpradid J, Kim IH, Staats HF, Haniffa M, MacLeod AS, Abraham SN, Perivascular dendritic cells elicit anaphylaxis by relaying allergens to mast cells via microvesicles. Science. 362, eaao0666 (2018).

9. Ashina K, Tsubosaka Y, Nakamura T, Omori K, Kobayashi K, Hori M, Ozaki H, Murata T, Histamine induces vascular hyperpermeability by increasing blood flow and endothelial barrier disruption in vivo. PLoS One. 10 (2015), doi:10.1371/journal.pone.0132367.
10. Makabe-Kobayashi Y, Hori Y, Adachi T, Ishigaki-Suzuki S, Kikuchi Y, Kagaya Y, Shirato K, Nagy A, Ujike A, Takai T, Watanabe T, Ohtsu H, The control effect of histamine on body temperature and respiratory function in IgE-dependent systemic anaphylaxis. J. Allergy Clin. Immunol. 110, 298–303 (2002). [PubMed: 12170272]
11. Tan CL, Knight ZA, Regulation of Body Temperature by the Nervous System. Neuron. 98 (2018), pp. 31–48. [PubMed: 29621489]
12. Madden CJ, Morrison SF, Central nervous system circuits that control body temperature. Neurosci. Lett. 696 (2019), pp. 225–232. [PubMed: 30586638]
13. Takahashi TM, Sunagawa GA, Soya S, Abe M, Sakurai K, Ishikawa K, Yanagisawa M, Hama H, Hasegawa E, Miyawaki A, Sakimura K, Takahashi M, Sakurai T, A discrete neuronal circuit induces a hibernation-like state in rodents. Nature. 583, 109–114 (2020). [PubMed: 32528181]
14. Cho J, Ryu S, Lee S, Kim J, Kim HI, Optimizing clozapine for chemogenetic neuromodulation of somatosensory cortex. Sci. Rep. 10, 1–11 (2020). [PubMed: 31913322]
15. Gomez JL, Bonaventura J, Lesniak W, Mathews WB, Rodriguez LA, Ellis RJ, Richie CT, Brandon K, Dannals RF, Pomper MG, Bonci A, Michaelides M, Chemogenetics revealed: DREADD occupancy and activation via converted clozapine. Science (80-.). 357, 503–507 (2020).
16. DeNardo LA, Liu CD, Allen WE, Adams EL, Friedmann D, Fu L, Guenthner CJ, Tessier-Lavigne M, Luo L, Temporal evolution of cortical ensembles promoting remote memory retrieval. Nat. Neurosci. 22, 460–469 (2019). [PubMed: 30692687]
17. Sciolino NR, Plummer NW, Chen YW, Alexander GM, Robertson SD, Dudek SM, McElligott ZA, Jensen P, Recombinase-Dependent Mouse Lines for Chemogenetic Activation of Genetically Defined Cell Types. Cell Rep. 15, 2563–2573 (2016). [PubMed: 27264177]
18. Hrvatin S, Sun S, Wilcox OF, Yao H, Lavin-Peter AJ, Cicconet M, Assad EG, Palmer ME, Aronson S, Banks AS, Griffith EC, Greenberg ME, Neurons that regulate mouse torpor. Nature. 583, 115–121 (2020). [PubMed: 32528180]
19. Nakamura K, Morrison SF, A thermosensory pathway mediating heat-defense responses. Proc. Natl. Acad. Sci. U. S. A. 107, 8848–8853 (2010). [PubMed: 20421477]
20. Hoffman GE, Smith MS, Verbalis JG, c-Fos and related immediate early gene products as markers of activity in neuroendocrine systems. Front. Neuroendocrinol. 14, 173–213 (1993). [PubMed: 8349003]
21. Yang WZ, Du X, Zhang W, Gao C, Xie H, Xiao Y, Jia X, Liu J, Xu J, Fu X, Tu H, Fu X, Ni X, He M, Yang J, Wang H, Yang H, Xu XH, Shen WL, Parabrachial neuron types categorically encode thermoregulation variables during heat defense. Sci. Adv. 6, 9414 (2020).
22. Zhuang ZY, Xu H, Clapham DE, Ji RR, Phosphatidylinositol 3-kinase activates ERK in primary sensory neurons and mediates inflammatory heat hyperalgesia through TRPV1 sensitization. J. Neurosci. 24, 8300–8309 (2004). [PubMed: 15385613]
23. Rosenbaum T, Simon SA, TRPV1 Receptors and Signal Transduction. TRP Ion Channel Funct. Sens. Transduct. Cell. Signal. Cascades, 91–106 (2007).
24. Duo L, Wu T, Ke Z, Hu L, Wang C, Teng G, Zhang W, Wang W, Ge Q, Yang Y, Dai Y, Gain of Function of Ion Channel TRPV1 Exacerbates Experimental Colitis by Promoting Dendritic Cell Activation. Mol. Ther. - Nucleic Acids. 22, 924–936 (2020). [PubMed: 33251043]
25. Omari SA, Adams MJ, Geraghty DP, TRPV1 Channels in Immune Cells and Hematological Malignancies. Adv. Pharmacol. 79, 173–198 (2017). [PubMed: 28528668]
26. Bertin S, Aoki-Nonaka Y, De Jong PR, Nohara LL, Xu H, Stanwood SR, Srikanth S, Lee J, To K, Abramson L, Yu T, Han T, Touma R, Li X, González-Navajas JM, Herdman S, Corr M, Fu G, Dong H, Gwack Y, Franco A, Jefferies WA, Raz E, The ion channel TRPV1 regulates the activation and proinflammatory properties of $CD4^+$ T cells. Nat. Immunol. 15, 1055–1063 (2014). [PubMed: 25282159]
27. Kügler S, Kilic E, Bähr M, Human synapsin 1 gene promoter confers highly neuron-specific long-term transgene expression from an adenoviral vector in the adult rat brain depending on the transduced area. Gene Ther. 10, 337–347 (2003). [PubMed: 12595892]

28. Chan KY, Jang MJ, Yoo BB, Greenbaum A, Ravi N, Wu WL, Sánchez-Guardado L, Lois C, Mazmanian SK, Deverman BE, Gradinaru V, Engineered AAVs for efficient noninvasive gene delivery to the central and peripheral nervous systems. Nat. Neurosci. 20, 1172–1179 (2017). [PubMed: 28671695]
29. Roth BL, DREADDs for Neuroscientists. Neuron. 89, 683–694 (2016). [PubMed: 26889809]
30. Amadesi S, Nie J, Vergnolle N, Cottrell GS, Grady EF, Trevisani M, Manni C, Geppetti P, McRoberts JA, Ennes H, Davis JB, Mayer EA, Bunnett NW, Protease-Activated Receptor 2 Sensitizes the Capsaicin Receptor Transient Receptor Potential Vanilloid Receptor 1 to Induce Hyperalgesia. J. Neurosci. 24, 4300–4312 (2004). [PubMed: 15128844]
31. Baral P, Udit S, Chiu IM, Pain and immunity: implications for host defence. Nat. Rev. Immunol. 19, 433–447 (2019). [PubMed: 30874629]
32. Bunker CB, Cerio R, Bull HA, Evans J, Dowd PM, Foreman JC, The effect of capsaicin application on mast cells in normal human skin. Agents Actions. 33, 195–196 (1991). [PubMed: 1897439]
33. Forsythe P, Mast Cells in Neuroimmune Interactions. Trends Neurosci. 42 (2019), pp. 43–55. [PubMed: 30293752]
34. Beck SC, Wilding T, Buka RJ, Baretto RL, Huissoon AP, Krishna MT, Biomarkers in Human Anaphylaxis: A Critical Appraisal of Current Evidence and Perspectives. Front. Immunol. 10, 494 (2019). [PubMed: 31024519]
35. Nishio H, Takai S, Miyazaki M, Horiuchi H, Osawa M, Uemura K, Yoshida K, Mukaida M, Ueno Y, Suzuki K, Usefulness of serum mast cell–specific chymase levels for postmortem diagnosis of anaphylaxis. Int. J. Legal Med. 119, 331–334 (2005). [PubMed: 15735956]
36. Tchougounova E, Pejler G, Åbrink M, The chymase, mouse mast cell protease 4, constitutes the major chymotrypsin-like activity in peritoneum and ear tissue. A role for mouse mast cell protease 4 in thrombin regulation and fibronectin turnover. J. Exp. Med. 198, 423–431 (2003). [PubMed: 12900518]
37. Grimsey NJ, Trejo J, Integration of Endothelial Protease-activated Receptor-1 Inflammatory Signaling by Ubiquitin, doi:10.1097/MOH.0000000000000232.
38. Bahou WF, in *Platelets* (Academic Press, 2007), pp. 179–200.
39. Zheng Y, Liu P, Bai L, Trimmer JS, Bean BP, Ginty DD, Deep Sequencing of Somatosensory Neurons Reveals Molecular Determinants of Intrinsic Physiological Properties. Neuron. 103, 598–616.e7 (2019). [PubMed: 31248728]
40. Zeisel A, Hochgerner H, Lönnerberg P, Johnsson A, Memic F, van der Zwan J, Häring M, Braun E, Borm LE, La Manno G, Codeluppi S, Furlan A, Lee K, Skene N, Harris KD, Hjerling-Leffler J, Arenas E, Ernfors P, Marklund U, Linnarsson S, Molecular Architecture of the Mouse Nervous System. Cell. 174, 999–1014.e22 (2018). [PubMed: 30096314]
41. Kupari J, Usoskin D, Parisien M, Lou D, Hu Y, Fatt M, Lönnerberg P, Spångberg M, Eriksson B, Barkas N, Kharchenko PV, Loré K, Khoury S, Diatchenko L, Ernfors P, Single cell transcriptomics of primate sensory neurons identifies cell types associated with chronic pain. Nat. Commun. 12 (2021), doi:10.1038/s41467-021-21725-z.
42. Rogoz K, Aresh B, Freitag FB, Pettersson H, Magnúsdóttir EI, Larsson Ingwall L, Haddadi Andersen H, Franck MCM, Nagaraja C, Kullander K, Lagerström MC, Identification of a Neuronal Receptor Controlling Anaphylaxis. Cell Rep. 14, 370–379 (2016). [PubMed: 26748715]
43. Palaniyandi SS, Nagai Y, Watanabe K, Ma M, Veeraveedu PT, Prakash P, Kamal FA, Abe Y, Yamaguchi K, Tachikawa H, Kodama M, Aizawa Y, Chymase inhibition reduces the progression to heart failure after autoimmune myocarditis in rats. Exp. Biol. Med. (Maywood). 232, 1213–1221 (2007). [PubMed: 17895529]
44. Gu Q, Lee LY, Effect of protease-activated receptor 2 activation on single TRPV1 channel activities in rat vagal pulmonary sensory neurons. Exp. Physiol. 94, 928–936 (2009). [PubMed: 19429642]
45. Pinho-Ribeiro FA, Verri WA, Chiu IM, Nociceptor Sensory Neuron–Immune Interactions in Pain and Inflammation. Trends Immunol. 38 (2017), pp. 5–19. [PubMed: 27793571]
46. Shakmak B, Al-Habaibeh A, Detection of water leakage in buried pipes using infrared technology; A comparative study of using high and low resolution infrared cameras for evaluating distant

remote detection. 2015 IEEE Jordan Conf. Appl. Electr. Eng. Comput. Technol. AEECT 2015 (2015), doi:10.1109/AEECT.2015.7360563.

47. Nuñez-Borque E, Fernandez-Bravo S, Yuste-Montalvo A, Esteban V, Pathophysiological, Cellular, and Molecular Events of the Vascular System in Anaphylaxis. Front. Immunol. 13, 700 (2022).
48. Jin C, Shelburne CP, Li G, Potts EN, Riebe KJ, Sempowski GD, Michael Foster W, Abraham SN, Particulate allergens potentiate allergic asthma in mice through sustained IgE-mediated mast cell activation. J. Clin. Invest. 128 (2018), pp. 4742–4743. [PubMed: 30272582]
49. Heuberger DM, Schuepbach RA, Protease-activated receptors (PARs): Mechanisms of action and potential therapeutic modulators in PAR-driven inflammatory diseases. Thromb. J. 17, 1–24 (2019). [PubMed: 30651722]
50. Abraham SN, St. John AL. Mast cell-orchestrated immunity to pathogens. Nat. Rev. Immunol. 10 (2010), pp. 440–452. [PubMed: 20498670]
51. Sousa-Valente J, Brain SD, A historical perspective on the role of sensory nerves in neurogenic inflammation. Semin. Immunopathol. 40, 229–236 (2018). [PubMed: 29616309]
52. Wernersson S, Pejler G, Mast cell secretory granules: Armed for battle. Nat. Rev. Immunol. 14 (2014), pp. 478–494. [PubMed: 24903914]
53. Jensen-Jarolim E, Pali-Schöll I, Roth-Walter F, Outstanding animal studies in allergy I. From asthma to food allergy and anaphylaxis. Curr. Opin. Allergy Clin. Immunol. 17, 169–179 (2017). [PubMed: 28346234]
54. McLendon K, Sternard BT, Anaphylaxis. StatPearls (2021) (available at https://www.ncbi.nlm.nih.gov/books/NBK482124/).
55. Severe Allergic Reactions (Anaphylaxis) - Michigan Allergy & Asthma Specialists - Commerce Township, MI and Mount Clemens, MI, (available at https://michiganallergycenter.com/patient-education/anaphylaxis/).
56. Oreskovich SM, Ong FJ, Ahmed BA, Konyer NB, Blondin DP, Gunn E, Singh NP, Noseworthy MD, Haman F, Carpentier AC, Punthakee Z, Steinberg GR, Morrison KM, MRI Reveals Human Brown Adipose Tissue Is Rapidly Activated in Response to Cold. J. Endocr. Soc. 3, 2374–2384 (2019). [PubMed: 31745532]
57. Hori T, Capsaicin and central control of thermoregulation. Pharmacol. Ther. 26, 389–416 (1984). [PubMed: 6085515]
58. Gomtsyan A, McDonald HA, Schmidt RG, Daanen JF, Voight EA, Segreti JA, Puttfarcken PS, Reilly RM, Kort ME, Dart MJ, Kym PR, TRPV1 ligands with hyperthermic, hypothermic and no temperature effects in rats. Temp. Multidiscip. Biomed. J. 2, 297 (2015).
59. Ishii H, Sato T, Izumi H, Parasympathetic reflex vasodilation in the cerebral hemodynamics of rats. J. Comp. Physiol. B Biochem. Syst. Environ. Physiol. 184, 385–399 (2014).
60. Izumi H, Reflex parasympathetic vasodilatation in facial skin. Gen. Pharmacol. 26 (1995), pp. 237–244. [PubMed: 7590072]
61. Sheng Y, Zhu L, The crosstalk between autonomic nervous system and blood vessels. Int. J. Physiol. Pathophysiol. Pharmacol. 10, 17–28 (2018). [PubMed: 29593847]
62. Yang D, Luo Z, Ma S, Wong WT, Ma L, Zhong J, He H, Zhao Z, Cao T, Yan Z, Liu D, Arendshorst WJ, Huang Y, Tepel M, Zhu Z, Activation of TRPV1 by Dietary Capsaicin Improves Endothelium-Dependent Vasorelaxation and Prevents Hypertension. Cell Metab. 12, 130–141 (2010). [PubMed: 20674858]
63. Crane JD, Mottillo EP, Farncombe TH, Morrison KM, Steinberg GR, A standardized infrared imaging technique that specifically detects UCP1-mediated thermogenesis in vivo. Mol. Metab. 3, 490 (2014). [PubMed: 24944909]
64. Škop V, Liu N, Guo J, Gavrilova O, Reitman ML, The contribution of the mouse tail to thermoregulation is modest. Am. J. Physiol. - Endocrinol. Metab. 319, F438–F446 (2020).
65. Wang W, Li R, Miao W, ; Evans Cody, Lu L, Lyu J, Li X, Warner DS, Zhong X, Hoffmann U, Sheng H, Yang W, Development and Evaluation of a Novel Mouse Model of Asphyxial Cardiac Arrest Revealed Severely Impaired Lymphopoiesis After Resuscitation. J. Am. Hear. Assoc. J Am Hear. Assoc. 10, 19142 (2021).

66. Choi HW, Bowen SE, Miao Y, Chan CY, Miao EA, Abrink M, Moeser AJ, Abraham SN, Loss of Bladder Epithelium Induced by Cytolytic Mast Cell Granules. Immunity. 45, 1258–1269 (2016). [PubMed: 27939674]

67. Wolf FA, Angerer P, Theis FJ, SCANPY: Large-scale single-cell gene expression data analysis. Genome Biol. 19, 1–5 (2018). [PubMed: 29301551]

68. McInnes L, Healy J, Saul N, Großberger L, UMAP: Uniform Manifold Approximation and Projection. J. Open Source Softw. 3, 861 (2018).

69. Usoskin D, Furlan A, Islam S, Abdo H, Lönnerberg P, Lou D, Hjerling-Leffler J, Haeggström J, Kharchenko O, Kharchenko PV, Linnarsson S, Ernfors P, Unbiased classification of sensory neuron types by large-scale single-cell RNA sequencing. Nat. Neurosci. 18, 145–153 (2015). [PubMed: 25420068]

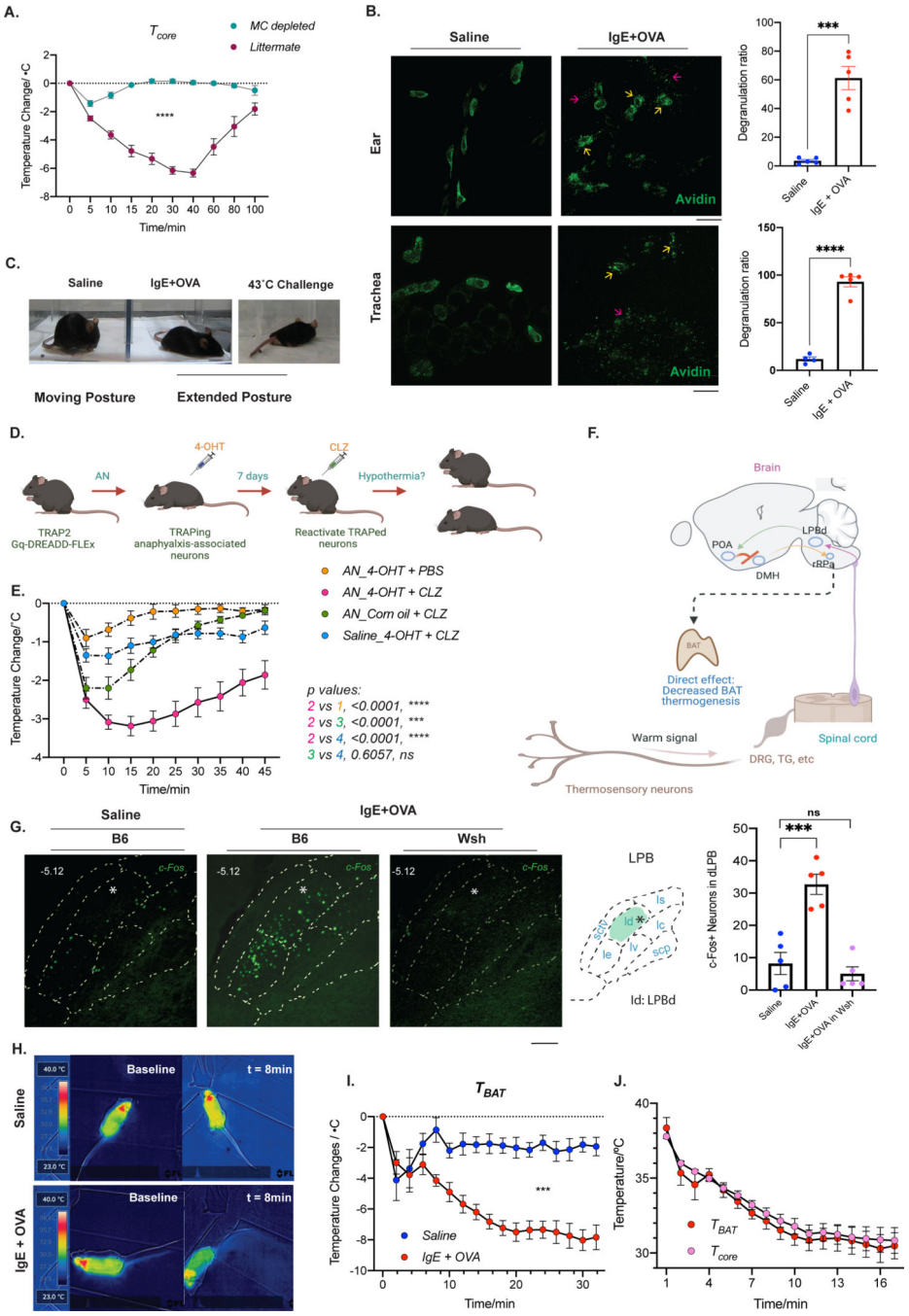

Figure 1. MC dependency and thermo-sensitive neural circuit activation during anaphylaxis.

(**A**) T_{core} of MC-depleted mice (*Mcpt5-iDTR*$^{+/-}$) and their littermates (*iDTR*$^{+/-}$) after the injection of TNP-OVA, n=4~46, two-way ANOVA. (**B**) MC degranulation in whole mount ears (**top**) and trachea (**bottom**) (t=10min) during acute anaphylaxis. MCs granules (Avidin, green); Yellow arrows: degranulating MCs; Magenta arrows: granules. Scale bar, 25μm. Degranulation ratio was graphed as the number of degranulated MCs/total MCs in the field, n=5 for ear, n=4 for trachea. Unpaired t-tests. (**C**) Left or Middle: Mouse behavior (saline or IgE-sensitized WT mouse) after injection of TNP-OVA. Right: Mouse behavior undergoing

heat challenge (43˚C ambient temperature). (**D**) A diagram showing the procedure for gaining genetic control over anaphylaxis-regulating neurons. (**E**) T_{core} in TRAPed or control mice after CLZ administration. 1. AN_4-OHT + PBS: TRAPed anaphylaxis mice injected with Saline; 2. AN_4-OHT + CLZ: TRAPed anaphylaxis mice injected with CLZ; 3. AN_Corn oil + CLZ: control mice injected with CLZ; 4. 4. Saline_4-OHT + CLZ: TRAPed control mice injected with CLZ. Two-way ANOVA, n=6~47). (**F**) A diagram showing the warm thermoregulatory neural circuit. Created with BioRender.com. (**G**) Left: representative images of LPBd (star*) neuronal activation staining (Bregma, −5.12mm). c-Fos, green. Scale bar, 100μm. Middle: a coronal view of LPB (green) with outlines of subregions. Right, quantification of numbers of c-Fos$^+$ neurons in LPBd. One-way ANOVA with Dunnett's multiple comparisons, n=5. (**H-J**) T_{BAT} changes in saline- or IgE-sensitized WT mice after TNP-OVA administration. (**H**) Representative infrared camera images at t=8min. (**I**) the quantification of T_{BAT} changes over time. (**J**) T_{BAT} and T_{core} dynamics presented in a single graph. Two-way ANOVA, n=5~46.

Data are presented as mean ± SEM. ns=p>0.05, ***p<0.001, ****p<0.0001. Two to three independent experiments were performed for each individual panel.

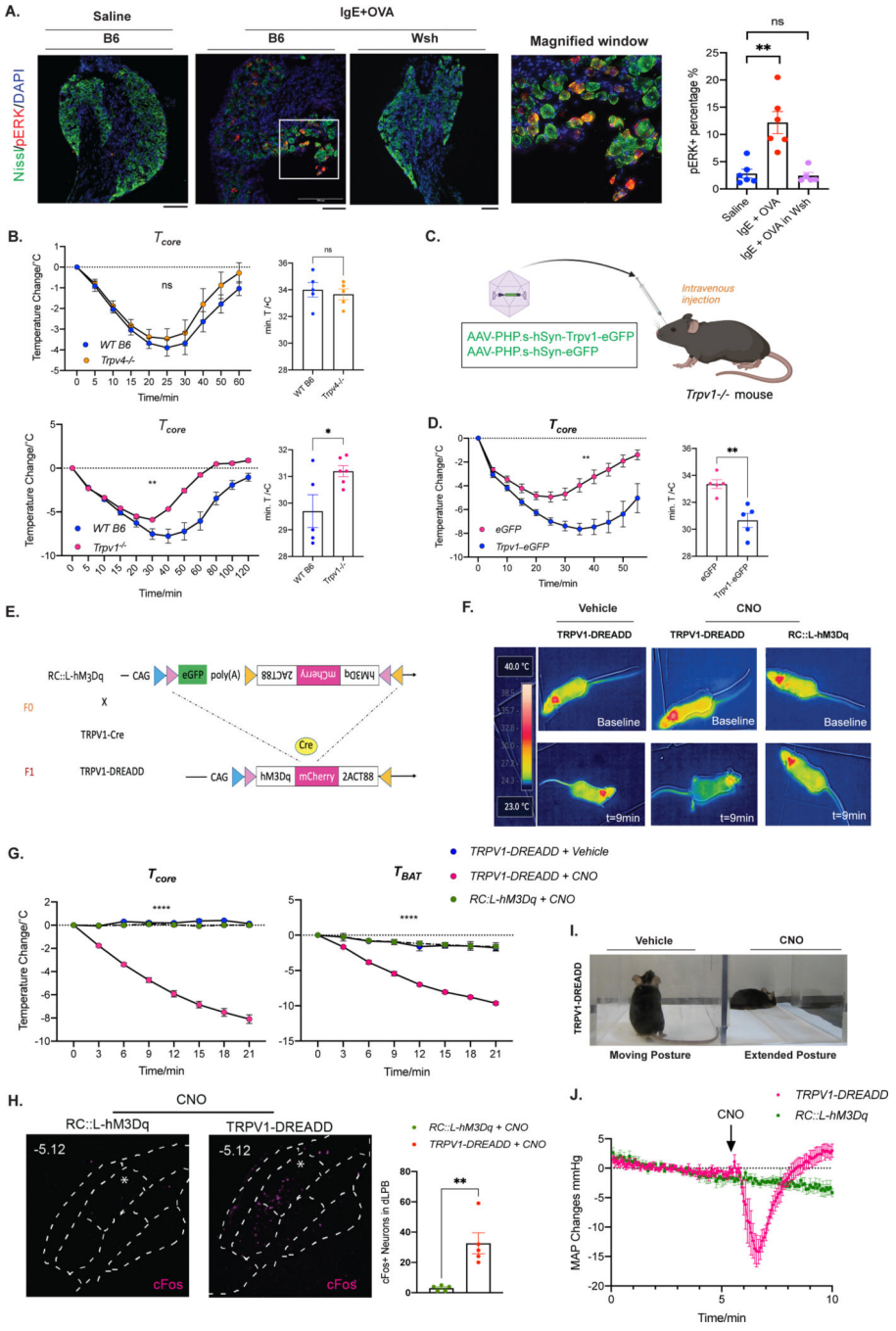

Figure 2. Systemic activation of TRPV1$^+$ sensory neurons inhibits BAT thermogenesis and contributes to the body temperature drop.

(**A**) **Left**: Representative images of sensory neuron activation staining with a zoomed-in window for the WT anaphylactic group. p-ERK, red; Nissl, green; DAPI, blue. Scale bar, 100μm. **Right**: p-ERK$^+$ neurons out of all neurons in DRGs. One-way ANOVA as global test, with unpaired t-tests as post hoc tests. N=5~46 mice. (**B**) T_{core} of *Trpv4*$^{-/-}$ (**top**) *and Trpv1*$^{-/-}$ (**bottom**) mice during anaphylaxis. Two-way ANOVA for T_{core} change graph, unpaired t-test for min T bar graph. N=5~46. (**C**) A diagram showing AAV-PHP.s-

hSyn-TRPV1-eGFP or AAV-PHP.s-hSyn-eGFP were intravenously (retro orbital injection) administered into 7-week-old *Trpv1*$^{-/-}$ mice. Created with BioRender.com. (**D**) T_{core} of *Trpv*1-rescued mice from (**C**) during anaphylaxis. Two-way ANOVA for T_{core} change graph, unpaired t-test for min T bar graph. N=5. (**E**) A diagram showing the genetics of TRPV1-DREADD mice. In TRPV1^{+} cells, eGFP is replaced by DREADD-mCherry expression due to the Cre recombinase activity. (**F-G**) T_{core} and T_{BAT} changes in TRPV1-DREADD and RC::L-hM3Dq mice after CNO (2 mg/kg) or vehicle control administration. (**F**) Representative infrared images at t=9min. (**G**) T_{core} changes, two-way ANOVA. (**H**) Left: Neuronal activation in LPBd region in TRPV1-DREADD and RC::L-hM3Dq after CNO administration. c-Fos, magenta; scale bar, 100μm. Right: quantification of numbers of c-Fos^{+} neurons in LPBd, unpaired t-test, n=5~46. (**I**) Mouse behavior in TRPV1-DREADD and RC::L-hM3Dq after CNO administration. (**J**) Mean arterial blood pressure (MAP) in TRPV1-DREADD and RC::L-hM3Dq in baseline (for initial 5min) and after CNO administration, n=4~45. Data are presented as mean ± SEM. ns=p>0.05, **p<0.01, ****p<0.0001. Two to three independent experiments were performed for each individual panel.

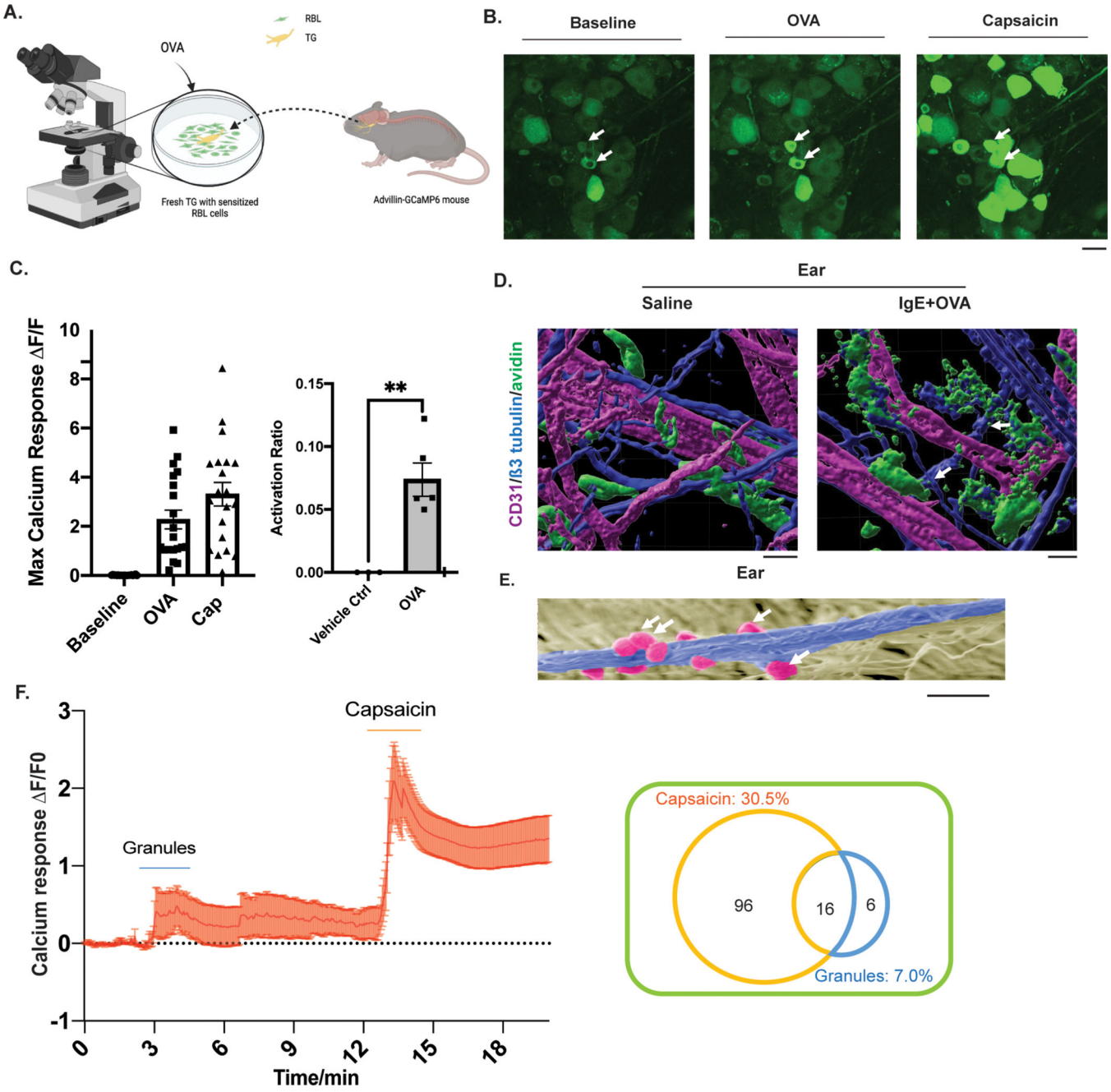

Figure 3. MC granules activate TRPV1^{+} sensory neurons.

(**A-C**) Calcium response of *ex vivo* TG neurons in responding to activated MCs. (**A**) A diagram showing fresh TGs were isolated from Advillin-GCaMP6 mice and then placed with IgE-sensitized RBL cells. Time-lapse imaging recorded TG neurons' response to 10ng/ml TNP-OVA activated RBL cells followed by 300nM capsaicin. Diagram was created with BioRender.com. (**B**) the representative images showing GFP intensity changes after treatments. White arrows point to the neurons that respond both to MC granules and capsaicin. Scale bar, 50μm. (**C**) the quantification of maximum calcium responses (ratios of fluorescence difference to the basal value) and the percentage of activated neurons as

the activation ratio, unpaired t-test. Four separate experiments were performed, 6 different Advillin-GCaMP6 mice were used.

(**D, E**) MC-released granules in whole mount ears from saline or IgE-sensitized WT mice 10min after TNP-OVA. (**D**) MC (Avidin, green), blood vessels (CD31, purple) and nerve fibers (ß3-tubulin, blue). White arrows point to the granules that fall off on the nerve fibers. Scale bar, 15 μm. (**E**) Pseudo-colored representative SEM image. Granules, magenta; representative nerve fiber, blue; background, light yellow. Scale bar, 2 μm. (**F**) Left: ratios of fluorescence difference to the basal value as the calcium responses. Right: Venn diagram showing the distribution of the activated DRG neurons and overlaps granule-responsive neurons and capsaicin-responsive neurons after granule application. The percentage of the activated population in cultured DRG neurons is indicated next to each chemical activator. Orange circle, the group of neurons responds to capsaicin; blue circle, the group of neurons responds to granule; center, the group of neurons which responds to both.

Data are presented as mean ± SEM. **p<0.01. Two to three independent experiments were performed for each individual panel.

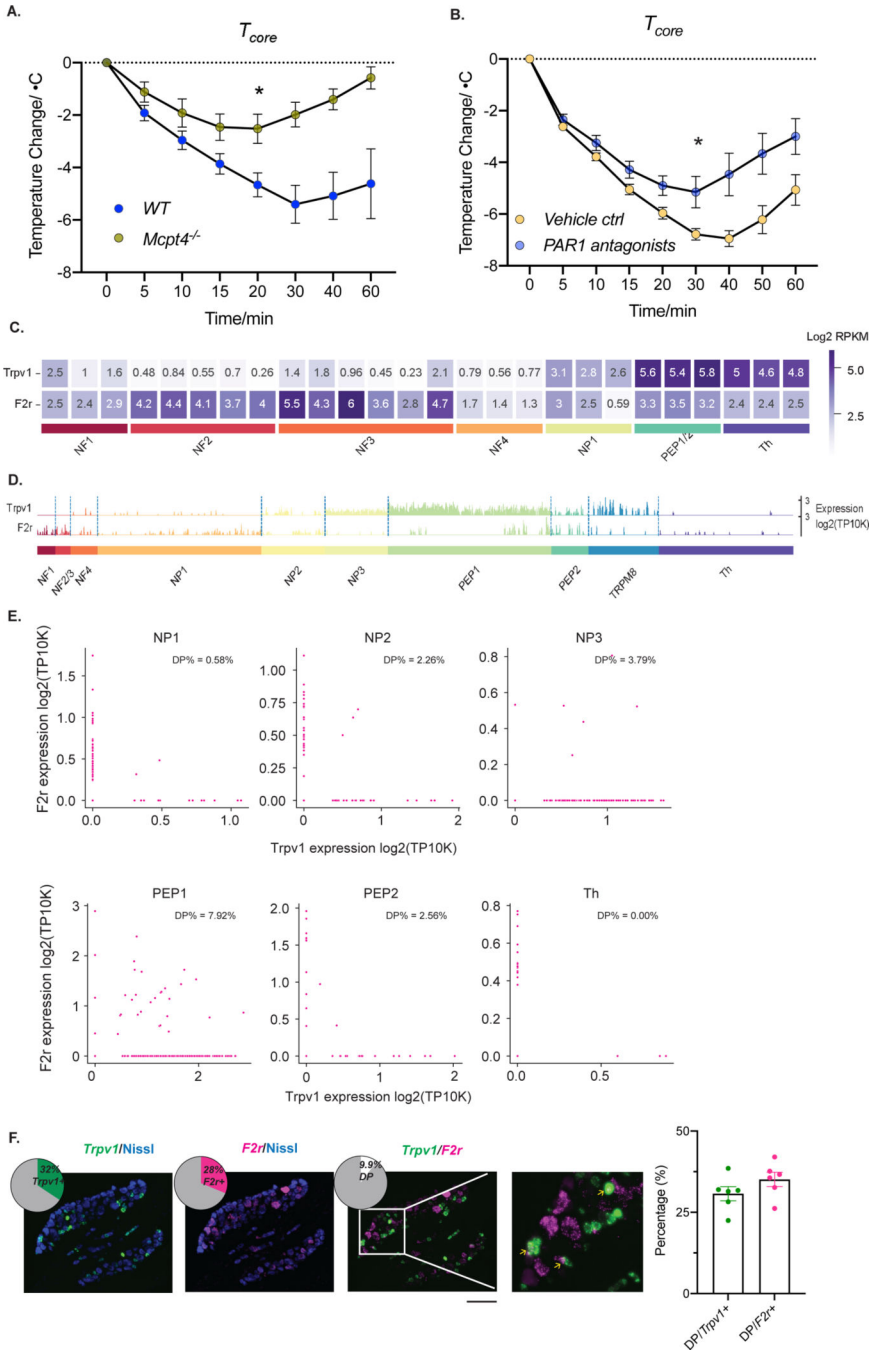

Figure 4. The specific contribution of chymase to anaphylaxis.

(**A**) T_{core} of IgE-sensitized *Mcpt4*$^{-/-}$ mice or WT after TNP-OVA administration, two-way ANOVA, n=5~46. (**B**) IgE-sensitized WT mice were treated with the combination of PAR1 antagonists RWJ 56610 (0.2mg/kg) and SCH 79797 (0.5mg/kg) or vehicle control 1h prior to the injection of TNP-OVA. Then T_{core} was monitored after TNP-OVA administration. Two-way ANOVA, n=6. (**C**) Heat map showing the average expression levels of *Trpv1* and *F2r* across mouse DRG neuronal cell types based on the bulk RNA-seq data produced by Zheng et al. (**D, E**) Analysis of mouse scRNA-seq data produced by Zeisel et al. (**d**)

Bottom: track plot showing the expression levels of *Trpv1* and *F2r* across mouse DRG single neuronal cells, grouped by predefined cell type. (**e**) *Trpv1* and *F2r* co-expressing mouse DRG single neuronal cells were plotted within each predefined cell type. DP (double positive) % on the top right of each plot is the percentage of *Trpv1* and *F2r* co-expressing cells out of total cells. (**F**) Representative RNAscope images of WT DRGs, *F2r* (Magenta) and *Trpv1* (Green), Nissl (Blue). From left to right: merge of *Trpv1* and Nissl; merge of or *F2r* and Nissl; merge of *Trpv1* and *F2r*. Scale bar, 100 μm. The zoomed-in inset shows a merge of *Trpv1* and *F2r*, in which arrows point to the *Trpv1* and *F2r* DP cells. The pie charts on the top-left of each image show the percentage of $Trpv1^+$ or $F2r^+$ or DP neurons out of total neurons. The bar graph on the right indicates the percentages of DP out of $Trpv1^+$ or $F2r^+$ neurons. Data are presented as mean ± SEM. *$p<0.05$. Two to three independent experiments were performed for each individual experimental result panel.

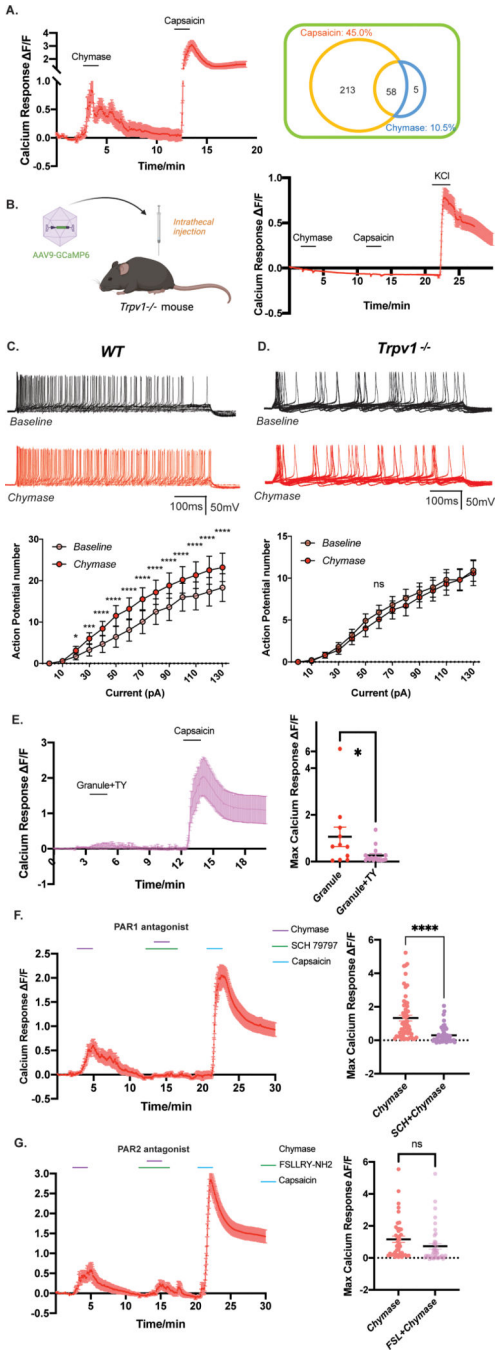

Figure 5. Chymase activates TRPV1^{+} sensory neurons through its cognate PAR1 receptor.

(**A**) Calcium responses of Advillin-GCaMP6 DRG neurons treated with 20 ng/ml chymase and followed by 300 nM capsaicin. Left: ratios of fluorescence difference to the basal value as the calcium responses. Right: Venn diagram showing the distribution of the activated DRG neurons and overlaps chymase-responsive neurons and capsaicin-responsive neurons after chymase application. The percentage of the activated population in cultured DRG neurons is indicated next to each chemical activator. Orange circle, the group of neurons responds to capsaicin; blue circle, the group of neurons responds to chymase; center, the

group of neurons which responds to both. (**B**) Calcium responses of *Trpv1*$^{-/-}$ DRG neurons treated with 20 ng/ml chymase and followed by 300 nM capsaicin. Left: a diagram showing that *Trpv1*$^{-/-}$ mice were intrathecally injected with ~41×10^{11}vg AAV9-GCaMP6 virus. Created with BioRender.com. Right: ratios of fluorescence difference to the basal value as the calcium responses were plotted. (**C, D**) Patch-clamp recordings in small diameter dissociated (**C**) WT DRG neurons or (**D**) *Trpv1*$^{-/-}$ DRG neurons with the application of 100 ng/ml chymase. Top: representative traces of current-evoked action potentials. Bottom: quantification of current-evoked action potentials. Two-way ANOVA as global test with Bonferroni's multiple comparisons test for difference under each individual current. n=10 neurons per group from 6 WT mice or 3 *Trpv1*$^{-/-}$ mice. (**E**) Calcium responses of Advillin-GCaMP6 DRG neurons responding to isolated MC granules + chymase inhibitor 50 nM TY 51469 (premixed with the granules 15 min before the experiment) and followed by 300 nM capsaicin. Left: Ratios of fluorescence difference to the basal value as the calcium responses were plotted. Right: the maximum of calcium responses to granule alone (Fig.3F) or the combination of granule + TY 51469, unpaired t-test. (**F, G**) Calcium influx in Advillin-GCaMP6 DRG neurons responding to chymase in the presence of PAR1 antagonist SCH 79797 or PAR2 antagonist FSLLRY-NH2. 20 ng/ml chymase at t=2~44min, followed by perfusion of (**F**) 1 μM SCH 79797 or (**G**) 10 μM FSLLRY-NH2 at t=12~415min, 20 ng/ml chymase was also given during t=13~414min. Later, t=20~422min, 300 nM capsaicin was added. Left: (**F**) 59 or (**G**) 41 representative calcium responses (the ratios of fluorescence difference to the basal value) of DRG neurons. Right: the maximum of calcium responses to chymase alone or chymase + individual antagonist, unpaired t-test. Data are presented in mean ± SEM, ns=p>0.05, *p<0.05. ***p<0.001, ****p<0.0001. Two to three independent experiments were performed for each individual panel.

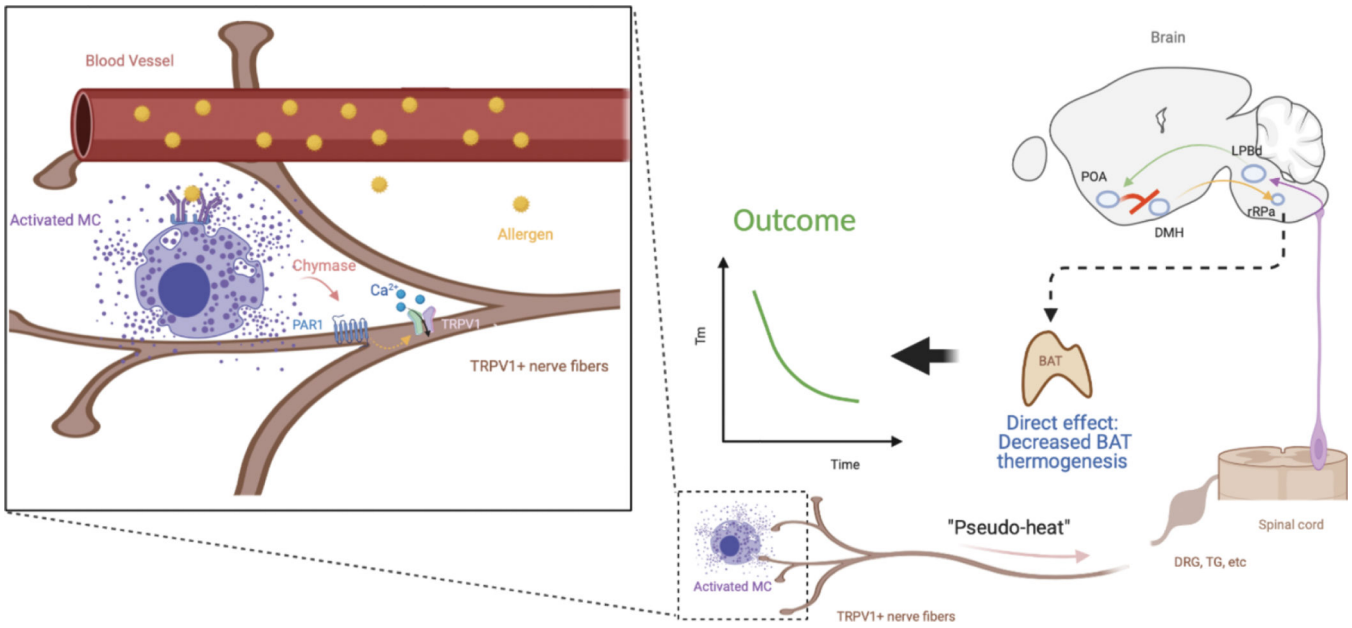

Fig 6. The summary model:

Left: a zoomed-in peripheral perivascular site. During IgE-mediated anaphylaxis, IgE-sensitized MCs are activated systemically when allergens bind to IgE, leading to extensive degranulation. Once released, granules fall on nearby nerve fibers, and this promotes the targeted release of multiple MC mediators to nerve fibers. Our study showed that one of the key proteinases in MC granules, chymase, can activate TRPV1^{+} sensory neurons through its cognate receptor PAR1. Right: MCs products activate TRPV1^{+} sensory neurons during anaphylaxis, triggering a pseudo-heat signal, which is transmitted through the warm thermoregulatory neural circuit (DRGLPBdMnPO), resulting in inhibition of BAT thermogenesis. This effect decreases heat production and contributes to hypothermia during anaphylaxis. Diagram was created with BioRender.com.